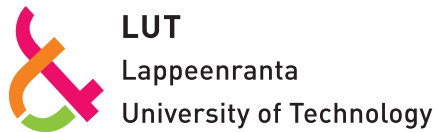


Acta Universitatis
Lappeenrantaensis
791



Jing Wu

**SOFT COMPUTING METHODS FOR
PERFORMANCE IMPROVEMENT OF EAMA
ROBOT IN FUSION REACTOR APPLICATION**



LUT
Lappeenranta
University of Technology



中国科学院大学
University of Chinese Academy of Sciences

Jing Wu

SOFT COMPUTING METHODS FOR PERFORMANCE IMPROVEMENT OF EAMA ROBOT IN FUSION REACTOR APPLICATION

Thesis for the degree of Doctor of Science (Technology) to be presented with due permission for public examination and criticism in the Auditorium room 2310 at Lappeenranta University of Technology, Lappeenranta, Finland on the 20th of March, 2018, at noon.

The thesis was written under a double doctoral degree agreement between Lappeenranta University of Technology, Finland and Institute of Plasma Physics Chinese Academy of Sciences, China and jointly supervised by supervisors from both Universities.

Acta Universitatis
Lappeenrantaensis 791

- Supervisors Docent Huapeng Wu
LUT School of Energy Systems
Lappeenranta University of Technology
Finland
- Professor Yuntao Song
Institute of Plasma Physics
Chinese Academy of Sciences
China
- Reviewers Professor Jouni Lampinen
Faculty of Technology, Computer Science
University of VASA
Finland
- PhD Luc Rolland
School of Engineering and Computing
University of West Scotland
UK
- Opponents Professor Jouni Lampinen
Faculty of Technology, Computer Science
University of VASA
Finland
- PhD Luc Rolland
School of Engineering and Computing
University of West Scotland
UK

ISBN 978-952-335-207-0
ISBN 978-952-208-7 (PDF)
ISSN-L 1456-4491
ISSN 1456-4491

Lappeenrannan teknillinen yliopisto
Yliopistopaino 2018

Abstract

Jing Wu

Soft computing methods for performance improvement of EAMA robot in fusion reactor application

Lappeenranta 2018

50 pages

Acta Universitatis Lappeenrantaensis 791

Diss. Lappeenranta University of Technology

ISBN 978-952-335-207-0, ISBN 978-952-335-208-7 (PDF), ISSN-L 1456-4491, ISSN 1456-4491

The experimental advanced superconducting Tokamak (EAST) has achieved a series of important research results and scientific discoveries. However, the EAST inner components of the first wall will also face an increasingly tough operating environment with high heat loads. Therefore, in order to ensure adequate running time, studying remote handling (RH) maintenance of the EAST device during physical experiments is a challenging task. The EAST's articulated maintenance arm system (EAMA) is developed for real-time detection and maintenance operations during plasma discharges without breaking the ultra-high vacuum conditions. To achieve the desired performance, EAMA must guarantee accuracy and stability. Building up the foundations needed for developing sensor fusion in a timely way can be facilitated by familiar hypothesis-driven or first principles approaches but also by engaging modern data-driven statistical methods. These methods feature machine learning (ML), an exciting R&D approach that is increasingly deployed in many scientific and industrial domains. An especially time-urgent and very challenging task in the development of intelligent RH services today is to reliably deal with large-scale major disruptions in magnetically-confined tokamak devices of the near future. Prediction methods with better predictive capability are required to provide sufficient advanced result for distribution mitigation or optimization strategies to be effectively applied to system remaining to be improved. This truly formidable task, outlined in this work, demands accuracy beyond the near-term reach of hypothesis-driven or first-principle simulations that dominate current research and development in the field. The ML methods deal with very large data sets hold significant promise for delivering the much-needed EAMA predictive tools that can be generalized at the basic level and used in multiple application domains. In particular, the signal data from the superconducting tokamak plasmas of high temperature (80-120°C), and high vacuum ($\sim 10^{-5}$ Pa), such as the EAST, is of significant interest to explore. In addition, the topic of vibration control, as an extension of our ML capabilities, is also a viable and timely subject to be studied. The main contributions of this dissertation include: the architecture, communication and model analysis of the entire EAMA software system; the optimization of EAMA trajectory by a genetic algorithm minimizing the end-point jerk; the study of two different methods, the extended Kalman estimator and the adaptive neural fuzzy system, to predict the pitch and yaw joint errors of the manipulator; and the eventual development of an estimation algorithm of EAMA dynamic vibration to predict the EAMA system operation.

Firstly, the design of the EAMA system should guarantee that the robot can stably run in the harsh environment of high temperature (80-120 °C) and high vacuum (about 10^{-5} Pa). The EAMA manipulator is a typical multi-body system; the overall speed is not high with an average joint angular velocity of about $\sim 0.5-1$ °/s. Meanwhile, the EAMA has a reduced structural stiffness and strictly limited operating speed. The inertial forces generated from acceleration could generate exaggerated, unwanted displacement and vibration. Any inappropriate motions can significantly cause system performance degradation by reducing positioning accuracy and aggravating the settling time which could result in system instability. To overcome the flexibility weakness of EAMA, a series of measures are taken to enhance the accuracy of EAMA in several fields: the mechanical flexibility of multi-body system dynamics, the accurate control in high performance systems, and the stability-optimized motion plan.

Secondly, we present a trajectory optimization method that pursues the stable movement of the 7-degree-of-freedom-articulated arm, which maintains the mounted inspection camera anti-vibration. Based on dynamics analysis, the trajectory optimization algorithm adopts multi-order polynomial interpolation in the joint space. The object of the optimization algorithm is to suppress the end-effector vibration by minimizing the root mean square value of jerk. The proposed solution has such characteristics that can satisfy kinematic constraints of EAMA's motion and ensure that the arm runs within the boundaries of absolute values of velocity, acceleration and torque. The genetic algorithm is employed to search for a global and robust solution of this problem by mapping a jerk transformation under 0.5 m/s^3 .

Thirdly, for sensors in the EAMA position control, two algorithms are implemented for estimating and compensating segment position error. For yaw joint, the error model uses curve fitting, which has unnegligible nonlinearities. The extended Kalman filter is adapted to make the segment position compensation error accurate based on the curve fitted model. For pitch joint, it has two distinct tasks, shaft rotation direction signal processing and discrete data classification. Meanwhile, the ideas of neural network and expert system are applied to complete these tasks respectively. In this part, the use of an adaptive neuro-fuzzy inference system for estimating the compensation error from an unformulated cluster of data forming a disclosed hysteresis loop. The experiment results have shown that the root mean squared error is significantly improved, and the final results satisfy the accuracy requirement of up to 0.02 degrees.

Finally, an open software architecture developed for the EAST articulated maintenance arm(EAMA) is described. In the control point of view, it offers robust and proper performance and an easy-going experience based on Open Robot Control Software (OROCOS). The software architecture is a multi-layer structure including: an end layer, an up layer, a middle, and a down layer. In the end layer, the components are defined off-line in the task planner manner. The distributed architecture of the control system associating each processing node with each joint is mapped to a component with all functioning features of the framework.

Keywords: EAMA manipulator, soft computing, accuracy improvement, error modelling, tolerance compensation, genetic algorithm, extended Kalman filter, Adaptive Neuro-fuzzy Inference System, software architecture, real-time control, OROCOS

Acknowledgements

The work presented in this thesis was carried out between 2015 and 2017 in ASIPP China and LUT, Finland. I gratefully acknowledge the following funding sources supporting my doctoral study in different stages: Finfusion education grant, university of science and technology of china, ASIPP. At the completion of my graduation thesis; I wish to express my sincere appreciation to all those who have offered me invaluable help.

Firstly, I would like to express my heartfelt gratitude to my supervisors, Prof. Huapeng Wu, Prof. Yuntao Song and Prof. Heikki Handroos. I am very grateful to my supervisors for providing me with the opportunity to study as a doctoral student in LUT, and for all their subsequent help: for organizing the financial support of my research; and for their inspiring guidance, valuable suggestions and constant encouragement throughout my studies.

Secondly, thanks are also due to my dissertation reviewers and opponents, Prof. Jouni Lampinen and Dr. Luc Rolland, for their constructive and insightful comments and suggestions, which were a great help and improved the quality of the dissertation considerably. A special thank goes to Mrs. Barbara Miraftabi, Mr. Peter Jones for help kindly help with the language of the dissertation. Her detailed comments and corrections improved the dissertation immeasurably.

Besides, it is my sincere pleasure to acknowledge many friends and colleagues who provided encouragement, knowledge and constructive criticism, and with whom I shared many enjoyable discussions and memorable moments: Mr. Yong Cheng, Dr. Kun Lu, Dr. Wenlong Zhao, Dr. Hongtao Pan, Ms. Binyan Mao, Dr. Shanshuang Shi, Ms. Sari Damsten, Ms. Päivi Nuutinen, Ms. Merilin Juronen, Ms. Saara merritt, to name only a few. I should also give my hearty thanks to Dr. Xiaochen Yang, Dr. Ming Li and Dr. Yongbo for their precious help in my daily life in Finland.

A sincere thanks to Finland: the country I deeply love from my heart: the country I take almost ten years to spend with: the country created immortality people and eternity spirits.

Lastly, I am deeply thankful to my family for their love and support! Without them, this dissertation would never have been written. I am greatly indebted to my father and my sister for their immense and constant understanding and support.

The last word of acknowledgement I have saved for my beloved husband, Zhonghui Yang, who have supported me for all these years. This dissertation can be a best gift for our upcoming babies.

Jing Wu
January 2018
Lappeenranta, Finland

Contents

Abstract

Acknowledgements

Contents

List of publications.....	11
1 Introduction.....	13
1.1 Background and motivation.....	13
1.2 Thesis Objectives.....	17
1.3 Contributions and outline.....	18
2 EAMA minimum jerk trajectory planning of motion control.....	21
2.1 Work space of EAMA.....	21
2.2 Path plan of EAMA.....	21
2.3 Approach of trajectory plan.....	22
2.4 Trajectory plan target of EAMA.....	23
3 EAMA Hybrid Model Software Calibration for Joint Position Disturbance.....	27
3.1 EAMA control system.....	27
3.2 Error sources.....	29
3.3 Approaches for the compensation of sensing error.....	30
3.4 Error estimator design.....	31
4 Open software architecture for EAMA.....	33
5 Summary of Publications.....	35
5.1 P-I: Genetic algorithm trajectory plan optimization for EAMA: EAST Articulated Maintenance Arm.....	35
5.2 P-II: Extended Kalman Filter Estimator with Curve Fitting Calibration of EAST Articulated Maintenance Arm Position Disturbance Compensation.....	35
5.3 P-III and P-V: Adaptive Neuro-fuzzy inference system based estimation of EAMA elevation joint error compensation.....	36
5.4 P-IV: Open software architecture for east articulated maintenance arm.....	36
6 Discussion of results.....	37
6.1 P-I: Genetic algorithm trajectory plan optimization for EAMA.....	37
6.2 P-II, P-III and P-V: EAMA Hybrid Model Software Calibration for Joint Position Disturbance.....	37
7 Conclusions and future works.....	39
7.1 Conclusions.....	39

7.2 Future Work.....	40
References.....	43
Appendix A: Data sheet of ADIS16209 and AS5047D.....	49
Publications	

List of publications

This thesis contains material from the following papers. The rights have been granted by publishers to include the material in dissertation.

- I. Wu, J., Wu, H., and Song, Y. (2016). Genetic algorithm trajectory plan optimization for EAMA:EAST Articulated Maintenance Arm. *Fusion Engineering and Design*, 109-111, pp. 700-706.
- II. Wu, J., Wu, H., and Song, Y. (2016). Extended Kalman filter estimator with curve fitting calibration of EAST Articulated Maintenance Arm position disturbance compensation. In: *Electronic Information and Communication Technology (ICEICT), IEEE International Conference on*, pp. 379 - 383. City: Harbin.
- III. Wu, J., Wu, H., and Song, Y. (2017). Soft Computing Methods Compensation for East Articulated Maintenance Arm Position Disturbance. In: *IEEE SENSORS 2017*, pp. 1-3. City: Glasgow.
- IV. Wu, J., Wu, H., and Song, Y. (2016). Open software architecture for east articulated maintenance arm. *Fusion Engineering and Design* , 109-111, pp. 474-479.
- V. Wu, J., Wu, H., and Song, Y. (2018). Adaptive Neuro-fuzzy Inference System Based Estimation of EAMA Elevation Joint Error Compensation. *Fusion Engineering and Design*, 126, pp. 170-173.

1 Introduction

Fusion offers a secure, long-term source of electric power without producing greenhouse gases, short-life radioactive waste recyclable within 100 years, inherent safety and an almost unlimited fuel supply. Nuclear fusion refers to the process by which two lighter atomic nuclei aggregate to form a heavier nucleus and a very light nucleus or particle. In the fusion process, the mass loss of the nucleus will be converted into a huge energy release. The deuteron and triton reaction results in continuous burn in energy stars. As the deuterium and tritium can be extracted from seawater, this fusion fuel is almost infinite on earth. Economic models indicate that plant reliability and output power are key parameters driving electricity production costs. Based on current estimates, the cost of generating electricity through nuclear fusion is predicted to be close to the cost of other options.

1.1 Background and motivation

Remote handling (RH) technology for fusion application has been a comprehensive development in nuclear engineering industrialization, proposed in the late period of the twentieth century (Tada, et al.1995). RH enables an operator to do manual handling work at a particular site without being physically present at that work site, but it always involves a human being in the process since it is technically not a fully automated process. The inspection robot of the international thermonuclear experimental reactor (ITER), i.e., the articulated inspection arm (AIA), was developed by the CEA (Commissariat à l'énergie atomique et aux énergies alternatives) within the European work programme framework. It is composed of five segments with eight degrees of freedom (DOF) and a total range of 8m. AIA aims to demonstrate the feasibility of a multi-purpose in-vessel teleoperated inspection system (Gargiulo, et al. 2008).

Developments and improvements have happened in the RH field. The RH system for Joint European Torus (JET) nuclear fusion experiment maintenance was another teleoperated maintenance device upgraded with high-levelled integration; it includes robotic devices, advanced computers, a virtual reality system, television and a wide range of special tools (Murcutt, et al. 2011). The conceptual design of the blanket maintenance system for the China fusion engineering testing reactor (CFETR) was proposed in 2015. The blanket RH system comprises three main sub-systems: the In-vessel maintenance system (IVMS), the lifting system and the blanket tool manipulator system (BTMS) (Wei, et al. 2015). Blanket maintenance between the docking station (hot cell building and tokamak building) and inside the vacuum vessel (VV) is implemented by RH systems and the vertical maintenance cask in tokamak building as well. The RH system is already an inextricable part of fusion engineering. The experimental advanced superconducting tokamak (EAST) (wang, et al. 2008) is similar to the ITER in terms of shape and equilibrium, but smaller and more flexible. It is one of a few international devices that can be an important experimental test bench for conducting the ITER related steady-state advanced plasma science and technology research.

Figure 1.1 shows the VV of EAST different from the ITER, which has a distinct feature: a non-circular cross-section. Being aimed at the long pulse plasma discharges, a series of experimental techniques have been developed for or improved on EAST in recent years, e.g., the EAST articulated maintenance arm (EAMA) is a teleoperated device developed for maintenance of EAST's VV.

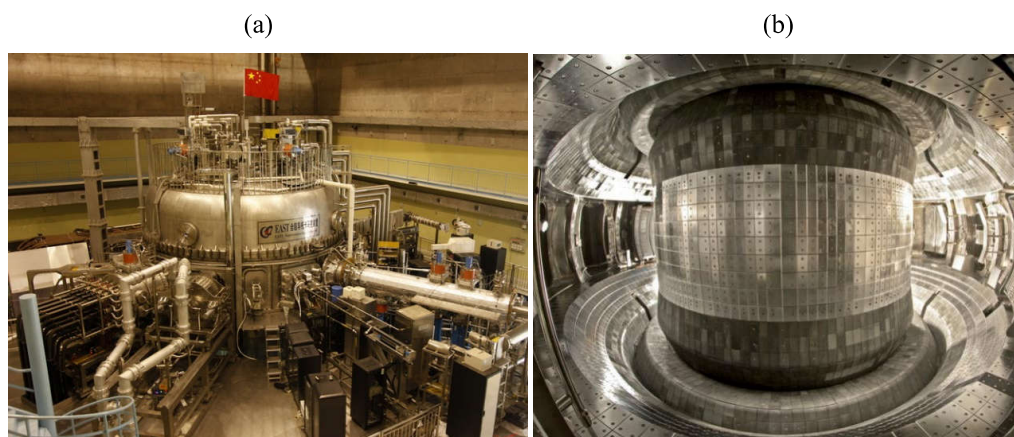


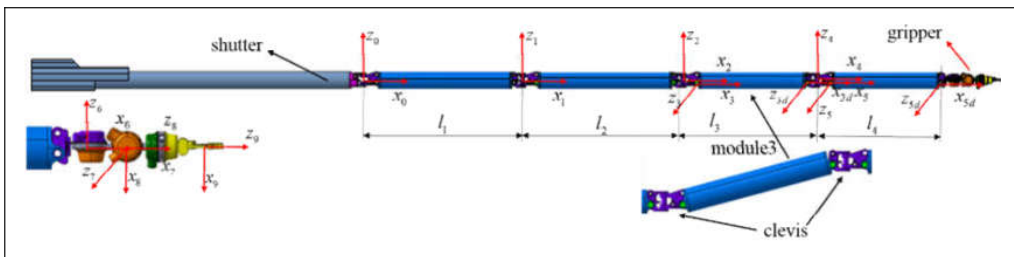
Figure 1.1 The EAST(a) EAST tokamak outlook, (b) EAST's vacuum vessel, EAST parameters ($R = 1.94$ m, $a = 0.45$ m), the equatorial port ($W \times H$, 528 mm \times 970 mm)

EAMA is not the first teleoperated device designed for EAST, the first in vacuum vessel inspection system (FIVIS) was proposed in 2010 for the hall inspection (Peng, et al. 2000) and basically presented requirements for the RH machines of EAST's in-vessel viewing system. The FIVIS system is composed of a limited number of fixed probes and is difficult to adequately cover all plasma facing components (Wang, et al. 2016). In contrast, EAMA operates embedded vision diagnostics allowing the interspace between components to be viewed. EAMA maintenance services include a geometrically enclosed space inspection task and a graphite tile friction-cleaning task for the plasma facing components (PFCs) of the EAST vessel. According to the task requirements of EAST VV, EAMA should be able to sustain the baking temperature (120°C) and vacuum (10^{-5} Pa). The positioning tolerance for clean graphite tile should be under 5mm for handling a payload that may reach a maximum of 2kg. Concurrently, for satisfactory machining vision diagnostics quality over the inspection area, the trajectory tracking accuracy of repeatability is expected to be under 0.5mm for the implemented machining work; and the workspace of the machining device should reach all the inner surfaces of the VV sector as much as possible. Meanwhile, the manipulator should smoothly move into the VV without any collision with the first wall. A security distance of 200mm is obtain, according to the maximum deflection of EAMA. (Shi. 2017).

In order to achieve this target, EAMA must possess multi-function capabilities, including integrating the vision tracking functions for PFC diagnostics (Yang, et al.

2016), assessing, adjusting, grasping functions of picking up broken graphite tiles and completing eradication. EAMA should be able to cover the whole area inside the EAST VV and produce a satisfactory operating result near the complex contoured inner surface of the VV sectors, except for some difficult areas near the entrance port and the conductor area of the equatorial ports. So a flexible redundant structure was adapted by EAMA with a total length of 8.8m and 10-DOF (Shi, et al. 2016). Table 1.1 gives the EAMA fundamental structure and functional requirements. The key requirements of high stability, high accuracy and high smooth performance have to be taken into account and embraced in the design of the EAMA system.

Table 1.1: EAMA structure and parameters



Designation:	Shuttle	S01	S02	S03	S04	Sd
Length(mm):	2630	1500	1500	1250	1250	520(700)
Axes 1:	linear translation	rotation +/- 90°				
Axes 2:	none	none	none	elevation +/- 45°	elevation +/- 45°	none
EAMA robot specifications	Vacuum: 10^{-5} Pa, -1atm Temperature: running: 80°C, baking: 120°C Workspace: R=1920, a=550mm DOF: 1 (base)+6 (arm)+3 (gripper) Payload: arm: 25kg manipulator: 2kg Dimension: radius: 160mm, length: 8.8m Weight < 100kg (arm) Function: inspection and pieces pickup					

To fulfil the objectives, a well-known parallelogram structure was adopted as the pitch mechanism of EAMA, as referenced in figure 1.2, where there are five bars: the horizontal rod, the robot tube, and two clevises. This parallelogram structure keeps the axis of the rotation joint vertical, produces a huge reduction ratio, and resists the strong torques generated from the long-reach arm gravity (Shi. 2017). Figure 1.3 illustrates the yaw mechanism which has two roller screw nuts with different lead directions driven by a brushless director current motor placed in a sealed box. The movement of the screwdriver is exported to the rotation joint by cables and a pulley system. The motion actuators are placed inside robot tubes, namely the rotation actuator is connected to the

tube while the elevation actuator is located diagonally to the mechanism. Consequently, each arm can be treated as a parallelogram mechanism.

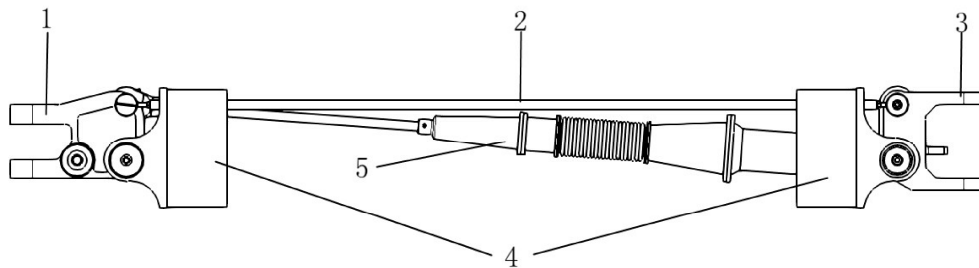


Figure 1.2 Parallelogram structure mechanism (Four bars: clevis 1, horizontal rod 2, clevis 3 and tube 4; pitch actuator 5).

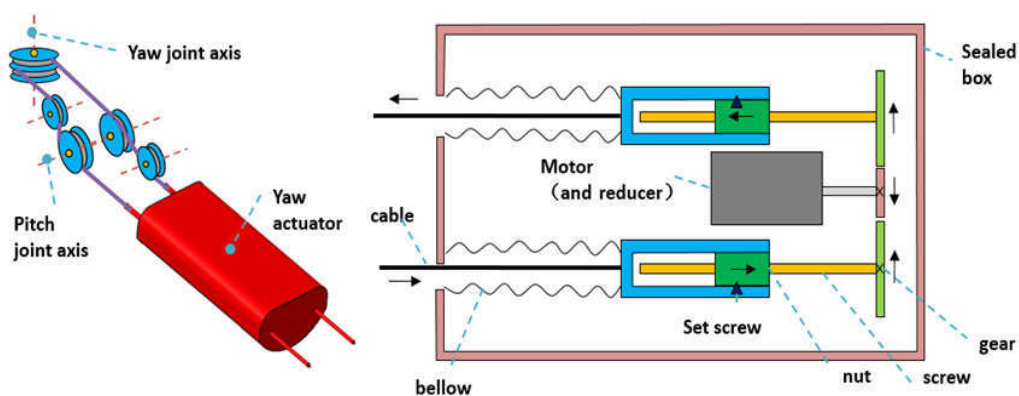


Figure 1.3 Movement diagram of the yaw actuator and pulley system.

The first version of EAMA was design in 2014 (Shi, et al. 2016), and it contained four segments. In 2015, the structure of EAMA was modified to be five segments for workspace accessing. Figure 1.4 is the final prototype of EAMA, where the blue segments contain only the yaw joint, and the red segments contain both yaw and pitch joints. EAMA has a reduced structural stiffness and strictly limited operating speed; the inertial forces generated from acceleration could generate exaggerated and unwanted displacements and vibration. Any inappropriate motions can significantly cause system performance degradation by reducing positioning accuracy and aggravating settling times (Wang, et al. 2016), e.g. system instability. In order to overcome the flexibility weakness of EAMA, a series of measures are managed to enhance the accuracy of EAMA in several fields: mechanical flexibility of multibody system dynamics (MSD), accurate control in high performance systems, and a stability optimized motion plan.

Recently, soft computing applications have been proposed to selectively expose hardware faults tolerances in the software layer (Thomas, et al. 2016). Genetic algorithm, neuro network, fuzzy system etc, these proposals algorithms are the keys of certain software applications to tolerate faults in their data, and still produce acceptable outputs. Soft computing applications have gained increasing prominence not only in

multimedia application, but also in industrial application (Dote, et al. 2001). Researchers have predicted that more modelling related work will belong primarily to this category (Witczak. 2007) . Examples of soft computing applications are prediction applications (Aminian, et al. 2017), which can tolerate noise, and optimization applications (Chandrasekaran, et al. 2010), which can offer a precise solution. These applications have an associated numerical objective, which is a quantitative measure of the output quality.

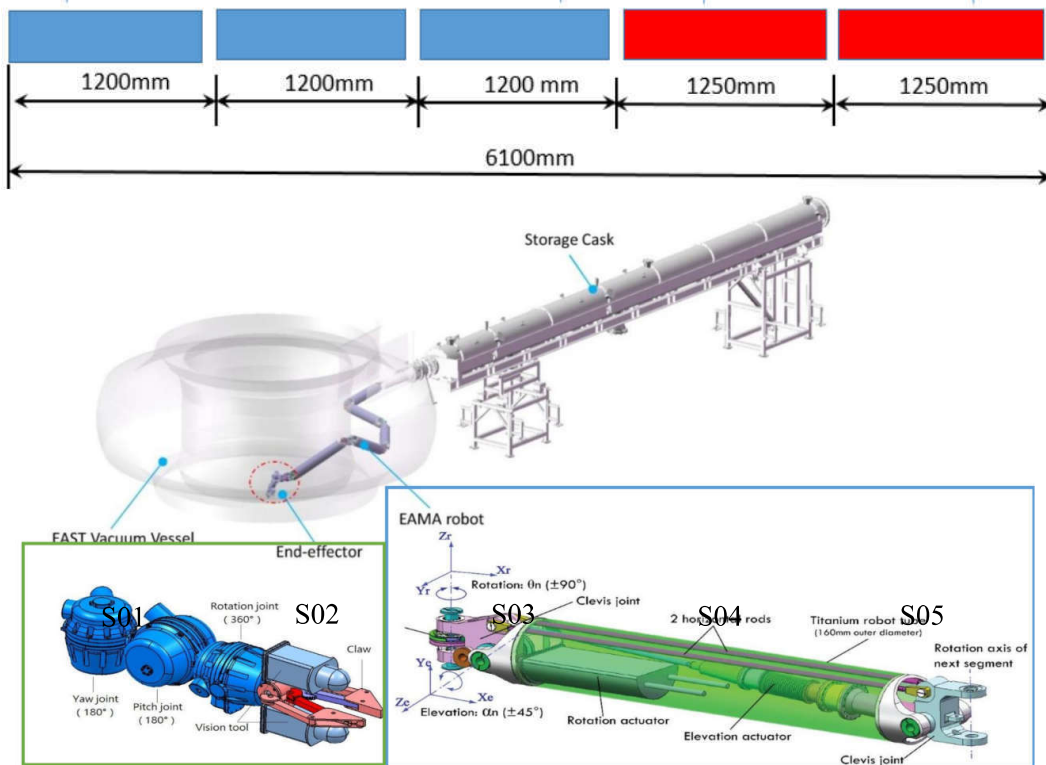


Figure 1.4 EAMA final configuration and laboratory work bench .

1.2 Thesis Objectives

The main objective of the study is to develop enhancing strategy for a serial-parallel kinematic redundant robot to improve the accuracy and vibration-reduced performance of the end-effector when performing the required tasks for EAST VV inspection and maintenance.

The elements of the desired strategy discussed in the thesis mainly encompass four aspects:

- Overview of EAMA

The construct and analysis of EAMA redundant articulated mechanisms, as well the operation requirement and techniques configuration with a flexible multibody approach. The environment conditions inside the vacuum vessel and given geometry are critical for EAMA development. These issues are described in detail first.

- End-effector jerk optimization trajectory plan

Smooth trajectory planning in the joint space along a prescribed geometric path for the end-effector of the robot. To avoid the singularity problem of redundant inverse kinematics for prescribed trajectories of the end-effector, a set of smooth trajectories is generated in the robot driving joint space. The performance of EAMA is taken as the optimization objective for the generation of joint trajectories so as to guarantee a precise movement performance.

- Sensor data fusion for position control of a parallelogram structure

To deal with the problem of joint error and sensor data fusion for the EAMA position control, the EAMA internal relative encoder is used for position control. Then, a compensator based on the corrected relative encoder and a novel algorithm is designed in a distributed manner. The estimated information is feed back to the desired poses for further speed and position control.

- An architectural approach of EAMA system

To develop a strategy using open software architecture for EAMA control, a robust, proper performance and easy-going experience is offered, based on a standard open-robotic software platform. The software architecture meets real-time demand, reliable communication and friendly user interface. The aim of the work is to obtain better RH performance to meet the demanding requirements of the EAST VV service tasks.

1.3 Contributions and outline

The following section presents the works carried out in this study.

The first part of work presents a trajectory optimization method aimed at the 7-DOF articulated arm with its stable movement to keep the mounted inspection camera still. Based on dynamics analysis, the trajectory optimization algorithm adopts a multi-order polynomial interpolation in joint space and a high order geometrical Jacobian transform. The object of the optimization algorithm is to suppress the end-effector movement vibration by minimizing the root mean square (RMS) value of jerk.

The proposed solution has characteristics that can satisfy the kinematic motion constraints of EAMA and ensure the arm will run according to the boundaries of absolute values of velocity. The genetic algorithm (GA) is employed to search for a global and robust solution to this problem.

For the sensors and sensor data fusion in the EAMA position control two algorithms are implemented to calibrate the yaw and pitch segment position error and estimate its signal. First, the extended Kalman filter is adapted to correct the segment position compensation error based on a curve fitted model.

Second, the adaptive Neuro-fuzzy Inference System is used to calibrate the pitch joint to estimate a compensation error from an unformulated cluster of data. The experiment result shows that the root mean squared error is significantly reduced, and the final results satisfy the accuracy requirement.

Finally, the concept framework of EAMA system is developed, the software application principle is indicated: the open architecture, the layers, the communication models, the user interfaces and the real-time operate system are analyzed and integrated. The hardware component and communication methods are indicated in detail as well.

The contents of this thesis are arranged as follows:

Chapter 2 presents EAMA minimum jerk trajectory planning of motion control.

Chapter 3 presents a hybrid model software calibration for joint position disturbance, the methods of a current control system, error sources and the most adaptable algorithm of an estimator.

Chapter 4 gives a suitable software architecture, software demands and an available solution are also described.

Chapter 5 provides summary of publications

Chapter 6 works on the discussion of results

Chapter 7 lists conclusions and future work suggestions.

Research publications are appended at the end of the thesis.

2 EAMA minimum jerk trajectory planning of motion control

2.1 Work space of EAMA

A most reasonable segment dimension has been calculated for the available space based on the geometrical characteristics of EAST vacuum vessel. The percentage of available space with respect to the entire EAST vessel is calculated as cloud volume divided by total volume of the fitting space. When the length has been decided as the dimension of EAMA robot, it reaches about 90% of available space.

Figure 2.1 illustrates the detailed calculation results for EAMA free space. According to the results, several conclusions can be indicated as follows:

- The robot can never get the space near entrance port.
- The available space can't guarantee 100%.
- The total length of robot mainly Influence the available space in the far end.

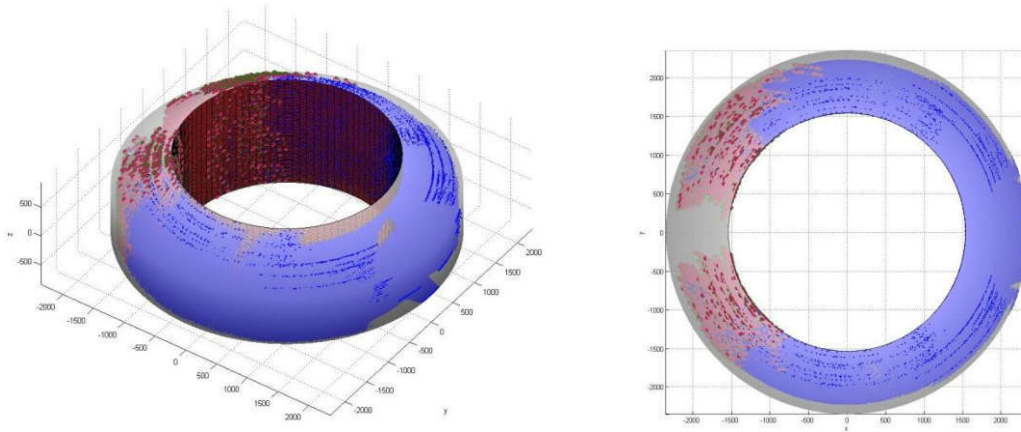


Figure. 2.1 General Cartesian workspace setting of EAMA.

2.2 Path plan of EAMA

In this closed ring space, the task area is divided into slices, and the joints of EAMA have very strict movement limitations. For a maximum visual view and travel clearance, the general path entering the VV is a concentric circle between the inner and outer edges of workspace. This guarantees that every segment completely enters the VV with joints cyclic of central point o (figure 2.2). After EAMA accesses the inspection area, the RH operation task defines the start and end points in the Cartesian space (Figure 2.3). The travel path of the end-effector can be protracted from the start point to the end point. Each joint value can be calculated via the inverse kinematics with respect to each pose of the end-effector.

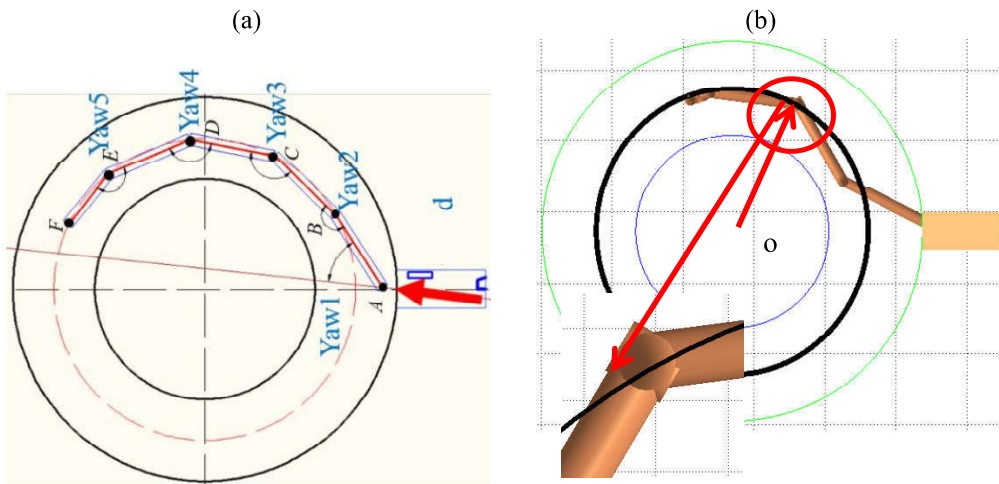


Figure 2.2 (a)EAMA completely entered displacement VV. (b) EAMA two segments entered displacement.

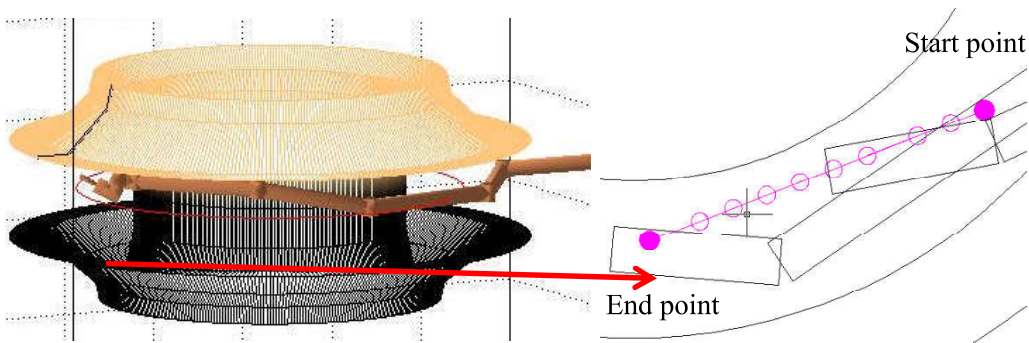


Figure 2.3 EAMA end point pose and the generated path in Cartesian space.

2.3 Approach of trajectory plan

Reasonable trajectory planning has become an important field in trajectory optimization. The minimum-time trajectory planning enhance robots efficiency (zhuang,et al, 2014). minimum energy trajectory planning is to plan the energy consumption according to the given points while the boundary constraints are satisfied (Gregory,et al,2012). Minimum vibration is an important performance positively impact the tracking accuracy, and many researchers have studied how to utilize minimum-jerk trajectory planning to reduce vibration(Gasparetto,et.al 2012). Research shows that trajectory planning of motion control could reduce vibration by preventing a discontinuous acceleration profile or a jerk. Two methods have been suggested: setting the minimum weighted sum of the integral squared jerk in Cartesian space, (Gasparetto, et al. 2010,2007) and

restricting the jerk value by adjusting the variance of the motion parameters (liu, et al. 2013, Bearee, et al. 2013). These algorithms have made it possible to set constraints on robot motion before execution and have been applied to improve practical performance. The main research procedure can be summarized as follows:

- The optimal objective function is transformed into a mathematical expression.
- Relational optimization methods are adopted to optimize the mathematical expression.
- The optimal results are indicated, and a conclusion is reached considering the requirements.

2.4 Trajectory plan target of EAMA

Trajectory planning can be defined as fulfilling a certain motion along a given geometric path and meeting the predefined demands. The ultimate aim of trajectory planning is to generate proper clues and suitable reference inputs for the control system of the robot. As shown in figure 2.4, when we have the information from current VV (vacuum vessel) environment and the task to be performed, the trajectory planner converts poses into movements according to desired motions, and the motion time of the trajectory is defined as the sum of the motion times of each segment. On another hand, the redundant structure of EAMA leads to many difficulties in solving singularity problems (Kim, et al. 1996). Some research work (huang, et al. 2007, Yue, et al. 2001) has focused on this issue in joint space by taking the kinematics redundancy of the flexible robots into account. For planning the joint trajectory of a multi-joint robot, the function of each joint angle is designed as a combination of preventing abrupt torque change and achieving smooth angular jerk (Constantinescu, et al. 2000), plus minimizing maximum jerk in the global view, which formalize the proposed trajectory as a global constrained optimization problem (Huang, et al. 2007, Huang, et al. 2006). The methods focus on single joint or joints but do not guarantee end-point performance of heavy coupled manipulators, especially in the case of a snake-like robot (Alambeigi, et al. 2014). Since the end-effector displacement is transformed from each joint with coupled structures, we restrict the joint jerk in a threshold, and expressed the constraints as the upper bounds on the absolute values of velocity and acceleration of the EAMA joints. The minimum jerk trajectory of the EAMA was evaluated in the end-effector with joint limitation. Therefore, jerk was calculated directly from the trajectory of the manipulator. Any physical limitations of the manipulator can be taken into account when the trajectory is being planned (Gasparetto, et al. 2008). After a set of knots (sequence of pose points) are designed in the joint space, interpolation can be done in two ways to approach blend segments: 1) the parametric evaluation (to blend from A to B over the course of several frames); and 2) the numerical integration (to blend one step forward from the current point to a tended point) (Acton, et al. 2012).

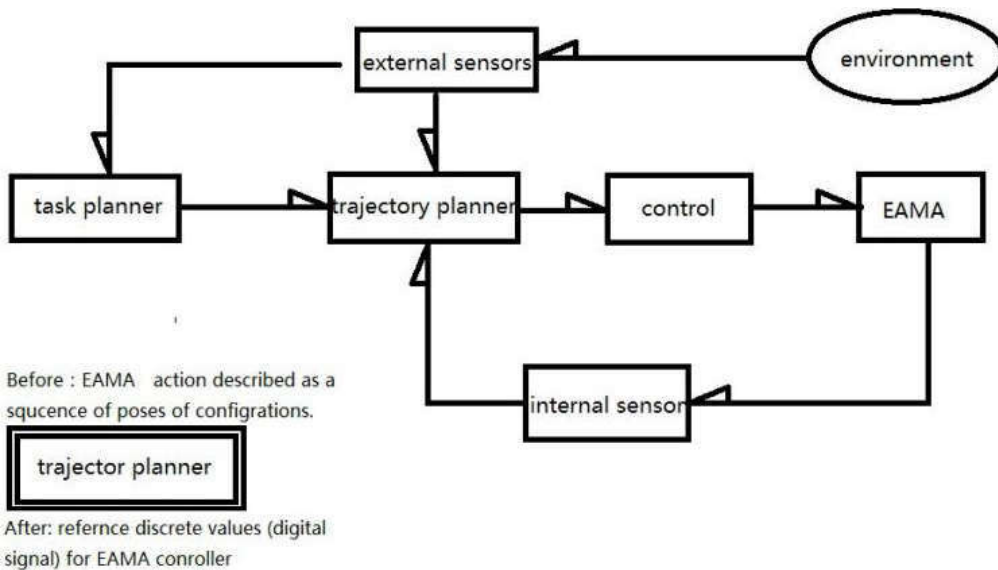


Figure 2.4 Block of EAMA general control system.

For an off-line model with inter knots, it is more convincing to use the parametric evaluation method. Spline interpolation takes several data points (knots) as inputs and interpolates the values for the segments between them. Cubic spline is the lowest-degree polynomial that can provide continuous acceleration and, in turn, a piece-wise constant jerk profile, which guarantees limited C^2 smooth trajectory (Aribowo, et al. 2014). Since jerk is the derivative of acceleration, the polynomial that can represent our desired parameters should at least have fourth order. But a higher order polynomial interpolation is not recommended because of local smoothness issues and coefficient solution problems (Guan, et al.2005), as below:

- N-th order polynomials have N-1 maximum and minimum points
- Oscillations arise out of the interpolation points (figure 2.5)

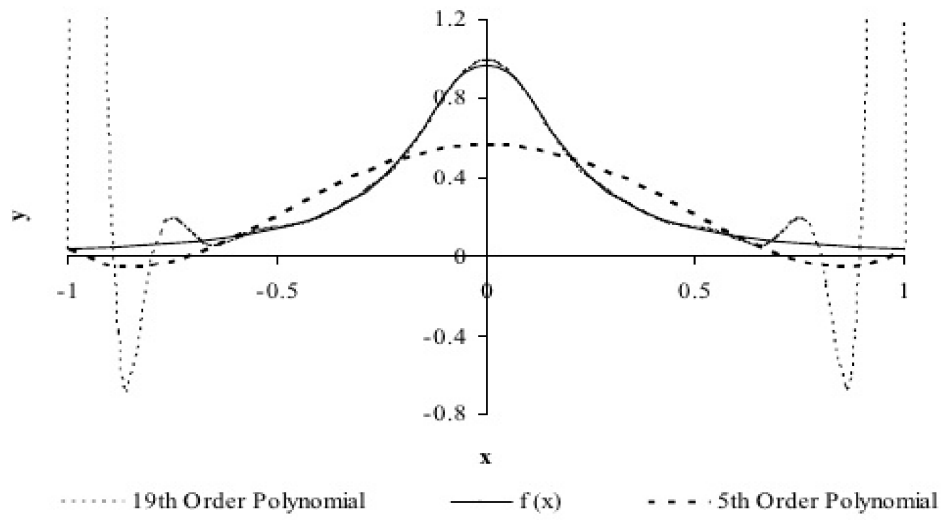


Figure 2.5 Different order of polynomial interpolation

3 EAMA Hybrid Model Software Calibration for Joint Position Disturbance

3.1 EAMA control system

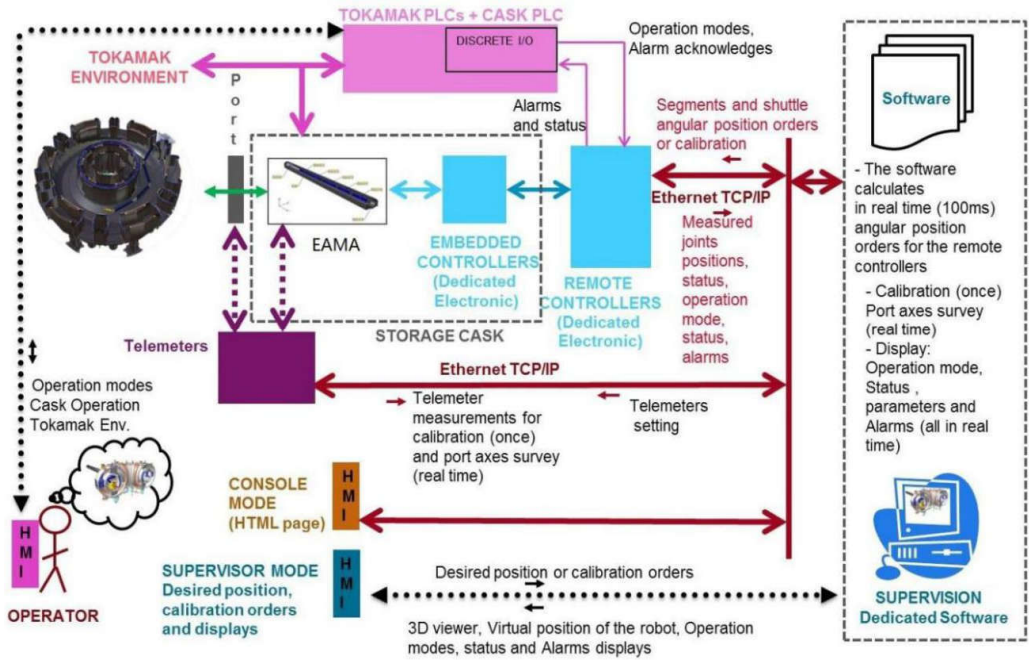


Figure3.1 Architecture of EAMA

In order to carry out servicing tasks remotely, manipulators require accurate feedback signals to ensure reliable operation control in the workspace (Virgala, et al. 2012). EAMA operates in a challenging environment not during nuclear fusion of vacuum pressure (10^{-5} Pa), high temperature (120°C) and high levels of radiation; consequently sensors need regular reassembly and reintegration to enable routine operations. Reassembly may introduce specific errors, which exacerbate uncertainty. Sensors used for the position feedback of the EAMA joint should have an accuracy higher than 0.14° (Pan, 2017). The flexible model, based on tests and combined with a position sensor and an inclinometer, can compensate any mechanical deformation. The aim of this work is to develop a high accuracy sensing system not only for surveying but also for compensation. Therefore, error compensation is required after data transmission. Figure 3.1 illustrates the architecture of EAMA, where hardware components, remote controllers and embedded controllers are responsible for low-level control of the manipulator. Remote controller is the control board, embedded controller is in charge of data collection and error compensation (figure 3.2).

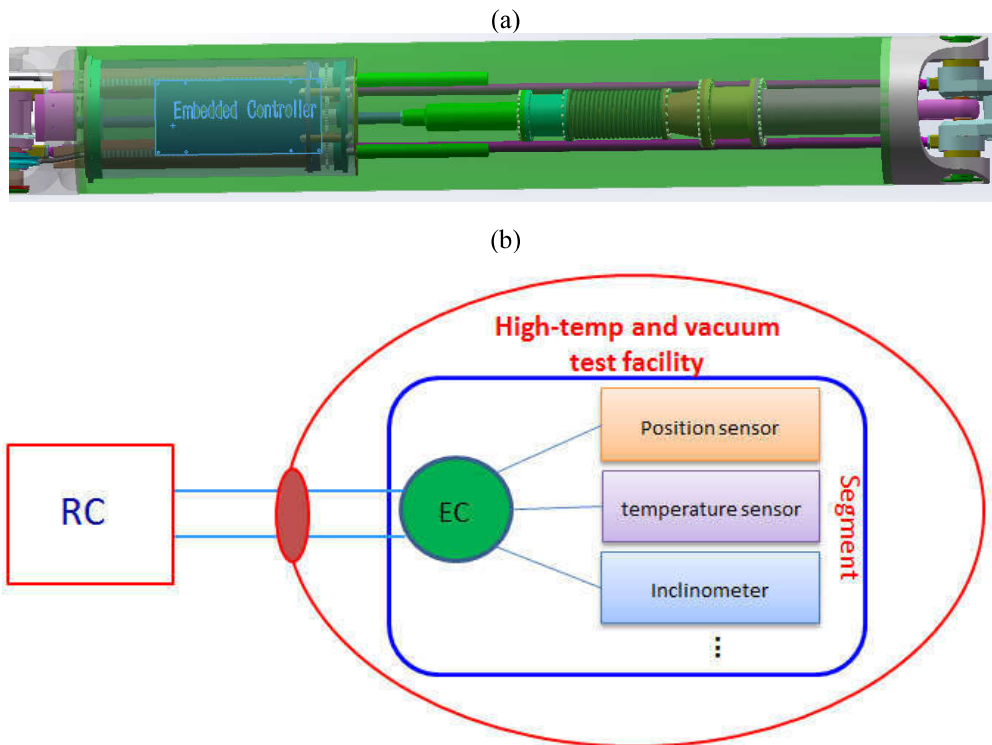


Figure 3.2. (a) Location of embedded controller in Segment 4; (b) Communication between RC,EC and sensors.

Sensors are integrated in each segment of the manipulator and connected to a CAN bus network. Remote controllers connect to the sensors through the CAN bus and communicate with the supervisor through the Ethernet.

During operation of the robot, each controller receives a position order every 100ms (a value that can be changed in the configuration file) even if a segment does not move. Each controller works in a positioning loop control (PID control) and receives a position order from the supervisor (Pan. 2017). The controller does not have to synchronize the relative movements of the different joints, since it is only in joint space. Each segment merely obtains the desired position from the supervisor allowing control of EAMA and transcribing it in real-time. The position orders for each remote controller have to be calculated in real time by the supervisor based on:

- The final position requested by the EAMA operator
- The current position of the robot by the values measured and sent via the remote controllers.

- The position of EAMA, computed by using the flexible model (Shi. 2017) or by the inclinometer values sent by the remote controllers.
- The environment, i.e., EAMA must not collide with the VV of tokamak, the storage cask.

When a capsule experiences a disturbance, software calibration needs to be carried out to compensate current position error. As shown in figure 3.2 (a)-(b), each segment joint of EAMA is equipped with an integrated sensor capsule containing a magnetic rotary position sensor. This position sensor is an electromechanical device that converts an angular position of the shaft or axle to the corresponding analog or digital code. Two integrated sensor capsules, A and B, are installed on the EAMA segment joint. Each capsule has one ADIS16209 (High-Accuracy, Dual-Axis Digital Inclinometer and Accelerometer) and one AS5047D position sensor. Capsule A is installed on the base clevis and Capsule B on the head clevis. A dual-mode inclinometer sensor in Capsule A can detect both the bending deformation and the torsion deformation of the segment. The inclinometer system in Capsule B is a redundancy design for elevation.

3.2 Error sources

The compact size encoder AS5047D is illustrated in figure 3.2 (b). The sensor microchip is fixed on the bearing housing and a magnet is attached to shaft. The magnet should be positioned centrally and aligned directly over the axis of the shaft. However, the gap between the inner ring and the outer ring introduces some discrepancy in assembly and axis alignment error. In addition to the mechanism arrangement effects, the sensor signal can be affected by electromagnetic compatibility disturbance (Kaminski, et al .2007), which can cause missing or extra counts in the signal. The mechanical factors causing erroneous signals include:

- Coupling is not tight and slipping.
- Slippage and tension when no belt is used.
- Incorrect wheel for the application or working incorrectly.
- Bad bearings cause roughness or side movement when turning the encoder shaft.

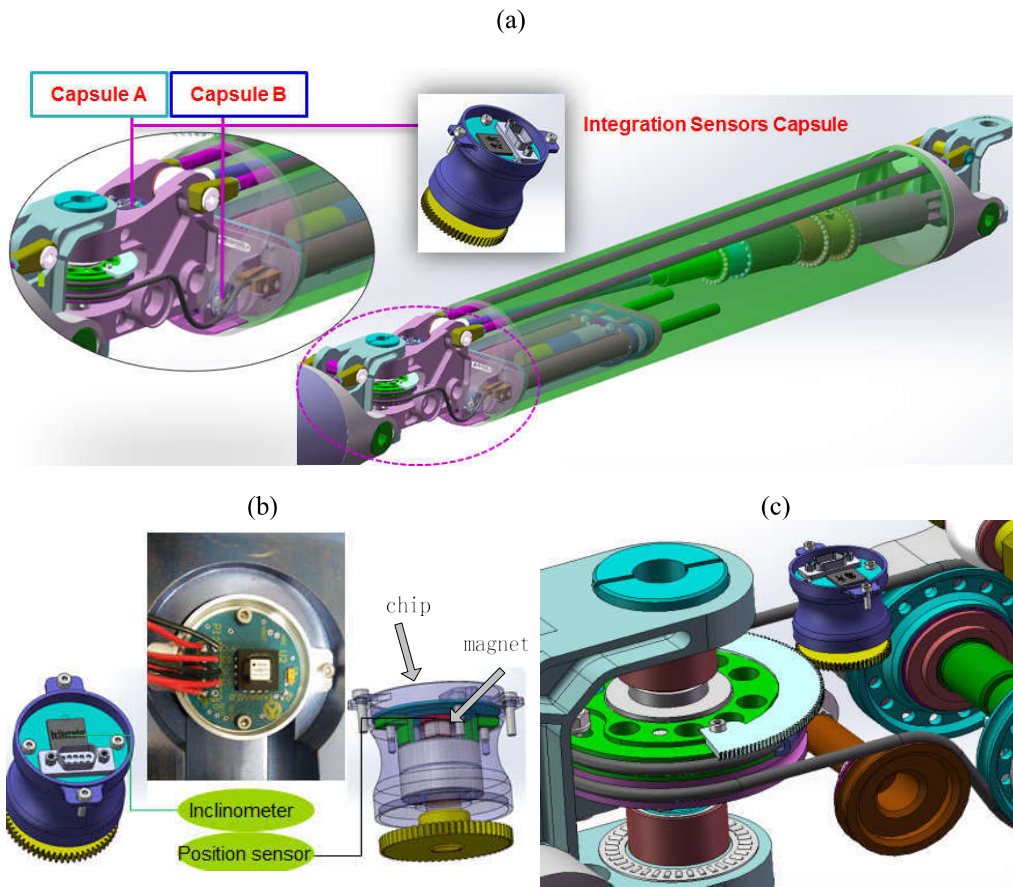


Figure 3.3. (a) Mechanism installation of the integrated sensor capsule in Segment 4; (b) AS5047D encoder accurate machine construction; (c) Perspective joint prototype.

3.3 Approaches for the compensation of sensing error

Several approaches exist for the compensation of sensing error: iterative algorithm methods (Dorveaux, et al. 2009); the use of assistant devices (e.g., a camera motion tracking system (Cooper, et al. 2009)); multi-sensor fusion measurement (Hol. 2011) (e.g., sensor data fusion for localization and position measurement (Eberhard, et al. 2013)); and physical adjustment (Hristoforou, et al. 1997). The very compact construction of EAMA precludes the use of limited assistant devices or multi-sensor fusion. Physical adjustment could overcome offset errors, but for high repeatability, a calibration table is barely enough since the errors are not always constant.

In light of the above constraints, software calibration would appear as the most appropriate solution among the currently available approaches. However, software

calibration requires filtering with a proper model, and the acquisition of a model from sensed results or deduced from all possibilities is not straight forward. Consequently, the use of intelligent hybrid systems is growing rapidly, and there are successful applications for process control, especially in model-less applications. In most cases, such systems can be employed to model nonlinear functions to estimate the nonlinear components on-line and to forecast chaotic time series. These systems would lead to significant improvement in control accuracy (Jang, 1993). In recent years, much research has been undertaken in areas such as sensorless estimation (Lima, et al. 2010), modeling hydrological time series (Nayak, et al. 2004), and model forecasting (He, et al. 2014, Kovac, et al. 2006).

3.4 Error estimator design

The error models for yaw and pitch joints have a distinguishing feature, namely, the period which is repeatable in continuous form or as a discontinuous hysteresis loop. Thus, it is difficult to apply one single estimator to achieve actualization and executability. In our case, the error model is not consolidated, and a multi-algorithm strategy should guarantee a unified accuracy criterion. To address executable and compatible issues, a parallel estimator is adopted in this work.

Extended Kalman filter (EKF) based solutions have been widely investigated for simultaneous estimation problems (Barut, et al. 2012, Akrad, et al. 2008). For nonlinear dynamic systems with unconstrained noise, the Kalman filter is extended by the system linearization of the near current parameter estimates. It updates parameters consistently with all previous measurement data and generally leads to convergence after a few iterations (Jiménez, et al. 2011). This approach is powerful, stable and efficient for nonlinear discretized state models. In our calibration application, the EKF is adopted to estimate the compensation error from an idealized curve-fitting model for the difference between the reference data and the experimental measurements. The proposed curve fitting method is based on the trust region reflective (TRR) least squares algorithm, which utilizes the multi-term sums of sine waves.

For elevation, we apply an adaptive neuro-fuzzy inference system (ANFIS) to model and forecast the compensation error from an unformulated data cluster. Fuzzy logic provides the mathematical ability to capture the uncertainties associated with cognitive processes that are difficult to acquire from incremental measurements. Artificial neural network (ANN) systems can be understood as simplified mathematical models of learning systems, and they work as parallel-distributed computing networks.

Table 3.1 presents a comparison of key features between the neural network and the fuzzy systems. It can be seen that neuro-adaptive learning techniques provide a method for fuzzy modelling procedures to learn information about data sets. Thus, fuzzy logic becomes capable of computing the membership function (MF) parameters that best allow the associated fuzzy inference system to track the given input and output data. The problem under study in this work comprises two distinct sub-tasks, shaft rotation

direction signal processing and serial data modelling. The neural network and expert system are investigated to solve these separate tasks respectively. ANFIS is a class of adaptive network, which is functionally equivalent to a FIS. The basics of ANFIS approaches are introduced in detail in many studies (Moon, et al. 2013, Jang. 1996, Depari, et al. 2007).

Table 3.1 Comparison between neural networks and fuzzy systems

<i>Neural Networks</i>	<i>Fuzzy Systems</i>
no mathematical model necessary	no mathematical model necessary
learning from scratch	priori knowledge essential
several learning algorithms	not capable of learning
black-box behavior	simple interpretation and implementation

4 Open software architecture for EAMA

EAMA software architecture covers subjects of task management, communication coordination, movement achievement, etc. The software is evaluated by multiple objectives during development, which includes schedulability, stability, portability and compatibility:

- **Schedulability:** the tasks can be scheduled in a deterministic way; for motion control of EAMA, real time schedulability is provided.
- **Stability/Robustness:** the software can tolerate failures in the individual tasks, and this is critical to the robot in a hostile environment.
- **Compatibility:** the software components are allowed to develop in a different software environment, such as in different languages. The components can be reused by one another.
- **Portability:** the software can be deployed in a different hardware environment. It also easily allows alien hardware to seamlessly join.

Beside the above demands, there are other functions required for the project application, and the user interfaces related to fusion engineering application are listed in table 4.1.

Table 4.1 Demand of software features.

Project application	User experience
Easy to migrate to other environments	Third-party expendable
Haptic device	3D mouse
Available library and standard support	3D Visualization
Fast develop period	Graphical interface
Easy to master code programming	Emergence button
Low budget software prototype	-----

Open Robot Control Software (OROCOS) is investigated with the requirements stated above. An open software architecture is convenient to reduce application budget and testing time, shorten the development period and realize portability. The OROCOS Real Time Toolkit (RTT) middleware provides utilities for communication and execution of

the components in real-time and guarantee schedulability; it merely occurs process crash. By using the scripting language, inexperienced programmers operation becomes easier. Enormous of libraries and standards offer variable control models and peripherals. They offer many accesses to GUI, visualization, control devices and plug-ins.

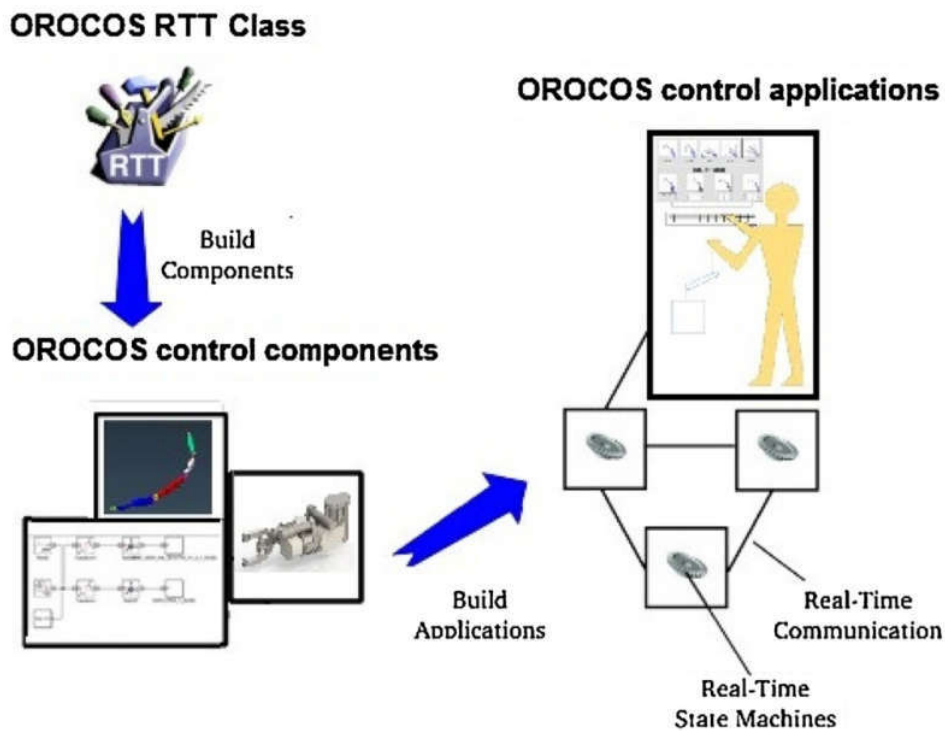


Figure 4.1 OROCOS distributed software development work flow.

The concept of component-based software design emphasizes the construction of systems using a number of software model classes (Zhang, et al. 2014) as shown in figure 4.1. When maximizing the efficiency of the entire application, different components should be able to exchange data and run in different applications. Each composition in the distributed environment shares data and resources; each component contains many models such as an algorithm model, a simulation model, an estimator model, a library model etc. (Bruyninckx, et al. 2001) These open source software packages are integrated with a massive operating system and an open standard Common Object Request Broker Architecture (CORBA) for internet communication.

5 Summary of Publications

This thesis, as a compendium, comprises five research publications; each one is briefly summarized below. Publications P-I - P-V deal with soft computing solutions for trajectory plans, joint error compensation and real-time software architecture.

5.1 P-I: Genetic algorithm trajectory plan optimization for EAMA: EAST Articulated Maintenance Arm

This paper introduces a trajectory optimization method which aims to provide the 7-DOF articulated arm with a stable movement keeping the mounted inspection camera anti-vibration. Based on dynamics analysis, a trajectory optimization algorithm utilizes multi-order polynomial interpolation in the joint space and high order geometry Jacobian transform has been studied.

The main contribution of this paper is that the optimization algorithm achieves the subject to suppress end-effector movement vibration by minimizing jerk RMS (root mean square) value of end effector. The proposed solution has characteristics that can satisfy kinematic constraints of EAMA motion and ensure the arm runs within the absolute values of velocity, acceleration and jerk boundaries. A GA (genetic algorithm) is employed to find a transmitted mapping solution under 0.5m/s^3 for a off-line joint space trajectory.

5.2 P-II: Extended Kalman Filter Estimator with Curve Fitting Calibration of EAST Articulated Maintenance Arm Position Disturbance Compensation

This paper implements an algorithm for the segment position error estimation and data compensation.

- First, the error model is curve fitted by TRR (trust region reflective) algorithm as 2 term Fourier series.
- Second, an extended Kalman filter is adapted to exact the segment position compensation error based on the curve fitted model.

The floating off-set can be canceled, but a part of disturbance and noise still remains. The simulation result shows that the root mean squared error is reduced from 0.03602 degrees to 0.0152 degrees, which provides significant improvement. Later in laboratory test yaw joint sensing satisfied the accuracy requirement of up to 0.02 degree.

5.3 P-III and P-V: Adaptive Neuro-fuzzy inference system based estimation of EAMA elevation joint error compensation

To achieve the correct link motion information, the measured signal from each joint sensor must be correctly mapped to the link motion. This paper implements the algorithms for calibrating and estimating the joint movements, i.e. using soft computing idea and adaptive neuro-fuzzy inference system to deal with the different joints that have different configurations was indicated in P-III. The T-S (Takagi-Sugeno) fuzzy model architecture is established. The emphasis of P-V is on the model computation and validation based on the previous work. The results show that joint position accuracy is significantly improved: minimum accuracy is 0.1degrees; repeatable accuracy is 0.05 degrees; and RSM accuracy is 0.02 degrees.

5.4 P-IV: Open software architecture for east articulated maintenance arm

In this article, an open software architecture developed for the EAST articulated maintenance arm (EAMA) is introduced. It is Based on a standard open robotic platform OROCOS and offers a robust, proper performance and easy-going functions. . The paper presents a component-based model software architecture using a multi-layer structure: end layer, up layer, middle, and down layer. In the end layer the components are defined off-line in a task planner manner. The components in the up layer complete the function of a trajectory plan.

The CORBA, as a communication framework, is adopted to exchange data between the distributed components. The contributors use the Real-Time Workshop from the MATLAB/Simulink to generate the components in the middle layer. The Real-Time Toolkit guarantees that the control applications run in real-time mode. Ethernet and CAN bus are used for data transfer in the down layer where the components implement hardware functions. The distributed architecture of the control system associates each processing node with each joint which are mapped to a component with all functioning features of the framework.

6 Discussion of results

6.1 P-I: Genetic algorithm trajectory plan optimization for EAMA

In this paper, the result of end-effector motion referring to movements of three segments is illustrated. GA obtained the best fitness value of end-effector jerk 0.22726 after 150 epochs. The goal of 0.5m/s^3 was achieved before 150 epochs, but the inter-knots are not necessarily calculated online.

The end-effector trajectory starts from the initial position, following the produced inter-knots, and reaches the destination; the detailed angle acceleration of end-effector motion in planner is optimized. the jerk of end-effector in Cartesian space is strictly limited. The target function implements inter-knots mapping strategy from complicated joint situation to the end-effector optimization goals. The GA algorithm can avoid calculating the jerk value transformed from each joint with coupled structure. Each joint satisfies the constraint requirements in joint space but not restrict as in global jerk minimum in Cartesian space.

6.2 P-II, P-III and P-V: EAMA Hybrid Model Software Calibration for Joint Position Disturbance

In our case, we trained individual models with different data sets to create diverse models so that their fusion would have a better accuracy than that of any single model. To improve the reliability of the controller by the error minimization approach, two estimators are used in a parallel structure and embedded in the control system.

After off-line training, the output values of the error model, generated by two different estimators, are applied as inputs to the servomotor of each pitch joint. An error vector is computed using the difference between the actual joint sensing data and the desired joint sensing results. The results are evaluated in the parallel estimator to generate the qualified results. The results are assigned to the controller for actual time steps; the output is assigned as the servomotor input of the joint. The plant and control system block of the estimators are shown in figure 6.1.

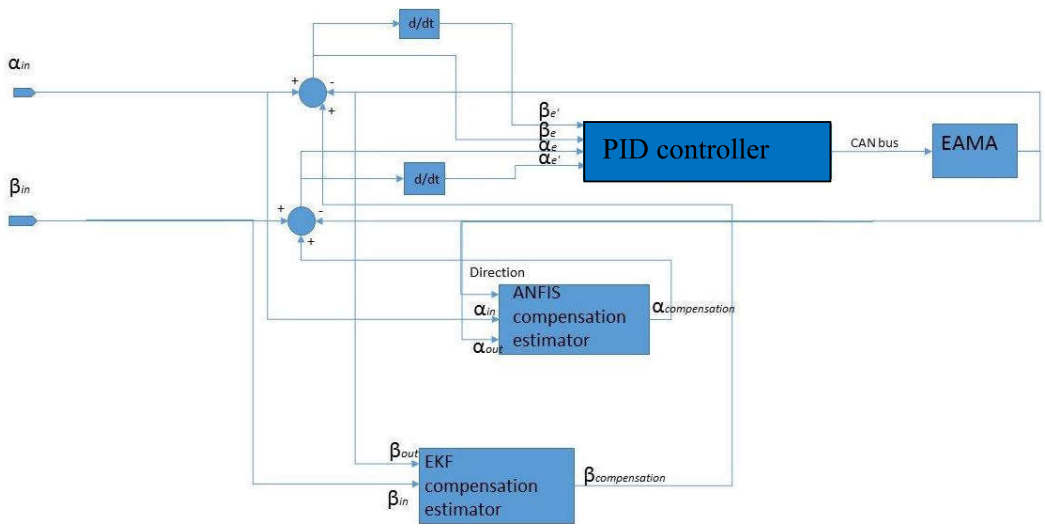
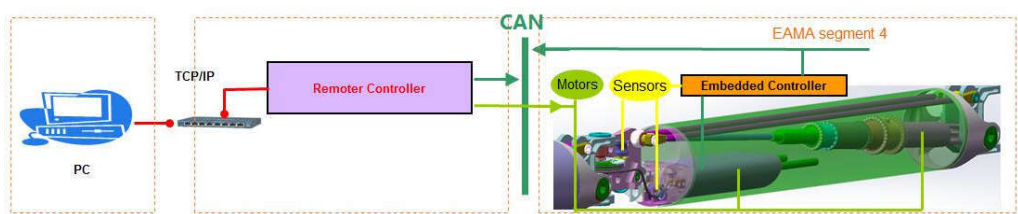


Figure 6.1 Block diagram of the parallel hybrid estimator.

Experiment results and laboratory test bench are shown in figure 6.2. The disturbance ripple of the yaw joint is reduced more significantly than the pitch joint, since the error modelling of the yaw joint is more benefit for curve fitting. But in both cases, satisfactory performance is demonstrated: maximum accuracy is 0.1° ; repeatable accuracy is 0.05° ; RSM accuracy is 0.02° . Solution performance requires estimation accuracy of compensated position disturbance below 0.14° .



Maximum Accuracy: 0.1°	Repeatability: 0.05°
RMS Accuracy: 0.02°	Test number: 50

Figure 6.2 Laboratory test bench for hybrid estimator and test result.

7 Conclusions and future works

7.1 Conclusions

In our approach, the two branches of soft computing applications (prediction and optimization) have been studied for EAMA accuracy improvement. First, we developed an algorithm to minimize the end-effector jerk movement for the multi-DOF manipulator EAMA. It provides optimal solutions by utilizing a genetic algorithm to find the root mean square value of jerk for a desired movement. The jerk results of the end-effector is successfully restricted in 0.5m/s^3 . The optimized motion trajectory in joint space not only can be used for model based dynamic control but can also be used as a good resource for robot vision. The method help to minimize self-disturbance and enhance the stability of EAMA.

Second, software sensor calibration is carried out, where there is limited tolerance with respect to cost and reliability. A data-driven model Extended Kalman estimator is applied to yaw joint calibration for tracking of errors and complementing errors compensation. This algorithm is also available as a hardware application (such as FPGA) (Pritsker, 2015), for a cheaper or less power consumption target. Meanwhile, ANFIS algorithm has been studied for joint error estimating. Compared to Extended kalman estimating method. ANFIS has many advantages in error estimation and sensor calibration, which can be concluded as follows:

- First, ANFIS architecture allows EAMA to easily incorporate with non-curve fitting model data calibrations and advance control algorithms.
- The training process usually only takes a few epochs to satisfy the accuracy requirement which shortens the calculation time.
- ANFIS models for various combinations of inputs can be trained with a single application for certain types of problems. Since the candidate inputs are divided into groups by a data structure, one or several members of each group can be added to the set of final inputs of the model, bringing greater flexibility to the sensor calibration factor. These members can even permit combination with other applications allowing fewer initial potential EAMA models to be built.

This work demonstrates that the two methods improve sensing accuracy and give better performance than the minimum requirement in terms of the reduction in position tracking errors of EAMA.

Third, we presents the conclusions of open software architecture for EAMA summarized as follows:

- First, this open software architecture allows EAMA to manipulate new task and algorithms by a component-based software.

- The connection between the simulator and EAMA is enhanced by employing real-time communication through open standard CORBA, RTAI with OROCOS RTT and the Real-Time Workshop from MATLAB/Simulink.
- Together with the component-based model and a distribution environment, a layered software structure has been proposed to embody the design. This structure imports a standardized interface that connects the components while allowing the developers to be distant. This feature causes the developed controllers more efficient and reliable.

7.2 Future Work

The mechanisms of EAMA are highly nonlinear and comprise coupled dynamics. As shown in figure 7.1(a), different schemes for pitch and yaw are actuated individually. The mathematical models of the manipulators are generally derived from energy principles: the rigid parts of 1n body and 2n upper rod store kinetic energy by their moving inertia and store potential energy by their position in the gravitational field. The flexible parts store potential energy by the deflections of their links, joints, or drives. When the gear modules have concentrated compliance, they can be modeled as pure springs storing only potential energy. Motion transformation mechanism components contain cables, screws and assistant springs which appear distributed with little kinetic energy due to their low inertia; a lumped parameter spring model works for potential energy replacement. In (b), tubes are subjected to torsion, bending, and compression. Torsion stores potential energy but little kinetic energy due to the low mass moment of inertia along the longitudinal axis of the beam and thus well represents a massless spring. Compression stores little potential energy due to high compressional stiffness, and the dynamics along this axis are often well described as rigid bodies. Bending stores potential energy by deflection as well as kinetic energy by deflection rates. To include bending, a cantilever beam equation with a point load at the end of beam could be applied. The original dynamics of EAMA, being described by partial differential equations, are not easily available for in both system analysis and control design.

However, dynamic couplings among the various kinematic chains of mechanisms, as well as between rigid body and flexible motions, are generally very complex in the modelling of EAMA. These couplings involve variable geometries resulting in varying system parameters. So, the motion equations are usually configuration-dependent for control purposes. In the model, which is the simplest for control purposes, EAMA could be modeled as a spring-mass system which does not often yield sufficiently accurate results. Obviously, reducing the complexity of the model needs certain assumptions leading to predictable errors. In addition to the difficulty of flexible links and joints in the combined model, we face the dilemma of technical feasibility.

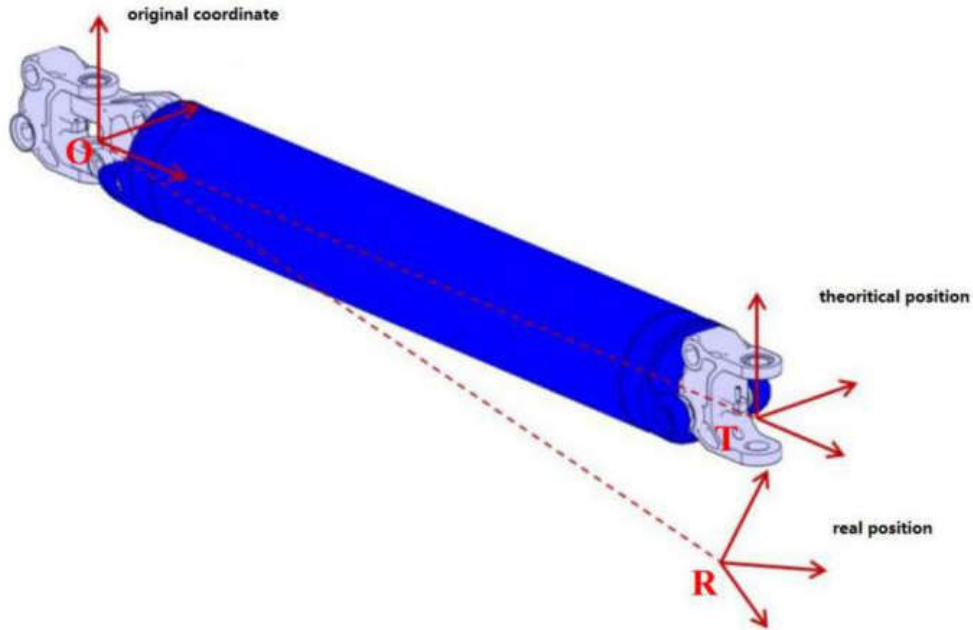
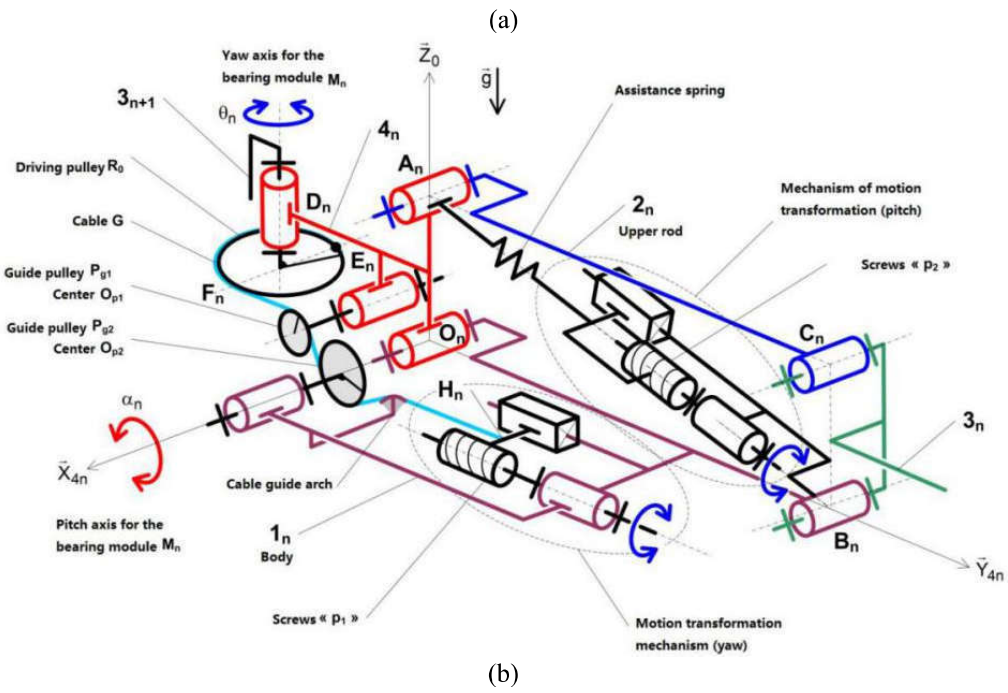


Figure 7.1. (a) Detail structure of EAMA single segment 4, (b) relative distribution.

- Sensors can not be inserted into torus and will not provide information at various rates; available communication has inevitable delay; hardware computation capability and the sensor fusion process are very limited.
- Flexible payloads cannot be accurately modeled in real time or at any effective fine motion control speed. For example, if gravity deflection is only 20 cm, the disturbance can lead to significant deflections that will not be supported by control methods.
- A structural simulator should be able to generate data at Hz scale.
- The deflection of the transporter is hard to distinguish in the joints or links, especially when a static joint behaves like part of an extended link.
- A real-size scale model should be available with guaranteed accuracy.

Assumptions and dependencies which are normally sufficient for engineering applications could fail in unexpected ways.

These are some reasons that compel us to discover new approaches to describe system behavior. Falling back on intelligent modelling techniques is an advisable option. In practice, models based on a combination of domain knowledge and training data are called grey-box models. Two main reasons cause inaccuracy in these models: simplifying assumptions and incomplete or inaccurate data. Mathematical models of complex systems are often simplified to reduce computational demands. Therefore, the underlying structure of the resulting models is no longer correct and structural errors are introduced into their predictions. It is usually impossible for the parameters of grey-box models to be determined from the material properties and other physical constants. If the system is information-poor, uncertainty associated with measurements and design data will be incomplete or inaccurate. As a result, the model will be calibrated correctly and parametric errors will be introduced into any model predictions. Therefore, based on the analysis of the previous sections, a new soft sensing methodology for dynamic vibration estimation will be proposed in the further research.

References

- Acton, M. (2012) Math for Game Programmers, *Sessions at GDC Game Developers Conference*.
- Akrad, A. Hilairet, M. Diallo, D. A (2008) sensorless PMSM drive with a two stage extended Kalman estimator. *IECON 2008. 34th Annual Conference of IEEE*.
- Alambeigi, F. Murphy, R.(2014) Control of the Coupled Motion of a 6 DoF Robotic Arm and a Continuum Manipulator for the Treatment of Pelvis Osteolysis. *36th Annual International Conference of the IEEE* ,pp.6521 - 6525.
- Aribowo, W. Terashima, K. (2014) Cubic spline trajectory planning and vibration suppression of semiconductor wafer transfer robot arm.*International Journal of Automation Technology*, 8(2), pp. 265–274.
- Barut, M. Demir, R. Zerdali, E. (2012) Real-Time Implementation of Bi Input-Extended Kalman Filter-Based Estimator for Speed-Sensorless Control of Induction Motors. *IEEE Transactions on Industrial Electronics*, 59(11), pp. 4197-4206.
- Bearee, R. Olabi, A. (2013) Dissociated jerk-limited trajectory applied to time-varying vibration reduction.*Robotics and computer-integrated manufacturing*, 29(2), pp. 444 - 453.
- Bruyninckx, H. (2001) Open robot control software: the orocos project IEEE international conference on robotics and automation. *Proceedings 2001 ICRA*, pp. 32523 - 2528.
- Chandrasekaran, M., Muralidhar, M., Krishna, C. M., Dixit, U. S. (2010). Application of soft computing techniques in machining performance prediction and optimization: a literature review. *International Journal of Advanced Manufacturing Technology*, 46(5-8), 445-464.
- Constantinescu, D. Croft, E. A. (2000) Smooth and Time-Optimal Trajectory Planning for Industrial Manipulators along Specified Paths.*Journal of Robotic Systems*, 17 (5), pp. 233-249.
- Cooper, G. Sheret, I. McMillan, L. Siliverdis, K. (2009) Inertial sensor-based knee flexion/extension angle estimation. *J. Biomechanics*, 42(16), pp.2678 - 2685.
- Dan, P. (2015). Hybrid implementation of Extended Kalman Filter on an FPGA. *Radar Conference (Vol.2015, pp.77-82)*. IEEE.
- Depari, A. Flammini, A. (2007) Application of an ANFIS Algorithm to Sensor Data Processing. *IEEE Instrumentation & Measurement Technology Conference*, 56(1), pp.75-79.

- Dorveaux, E. Vissière, D. A. Martin, J. (2009) Iterative calibration method for inertial and magnetic sensors. *48th IEEE Conference on Decision and Control and 28th Chinese Control Conference Shanghai, China*.
- Dote, Y. Ovaska, S. J. (2001). Industrial applications of soft computing: a review. *Proceedings of the IEEE*, 89(9), 1243-1265.
- Eberhard , P. Tang, Q. (2013) Sensor Data Fusion for the Localization and Position Control of One Kind of Omnidirectional Mobile Robots. *Multibody System Dynamics, Robotics and Control*. pp. 45-73.
- Gargiulo, L. Bayetti, P. Bruno, V, B. (2008) Development of an ITER relevant inspection robot. *Fusion Engineering and Design*, 83(10–12), pp.1833–1836.
- Gasparetto, A. Zanotto, V. (2008) A technique for time-jerk optimal planning of robot trajectories. *Robotics and Computer-Integrated Manufacturing*, 24(3), pp.415–426
- Gasparetto, A., & Zanotto, V. (2007) A new method for smooth trajectory planning of robot manipulators. *Mechanism and Machine Theory*, 42(4), pp.455-471.
- Gasparetto, A., & Zanotto, V. (2010) Optimal trajectory planning for industrial robots. *Advances in Engineering Software*, 41(4), pp.548–556.
- Gasparetto, A., Lanzutti, A., Vidoni, R., & Zanotto, V. (2012). Experimental validation and comparative analysis of optimal time-jerk algorithms for trajectory planning. *Robotics and Computer-Integrated Manufacturing*, 28(2), 164-181.
- Gregoryabb, J. (2012). Energy-optimal trajectory planning for robot manipulators with holonomic constraints. *Systems & Control Letters*, 61(2), 279-291.
- Guan, Y. Yokoi, K. Stasse, O. (2005) On robotic trajectory planning using polynomial interpolations. *IEEE Transl. J. Robotics and Biomimetics*, pp.111-116.
- He, Z. Wen, X. Liu, H. Du, J. (2014) A comparative study of artificial Neural network, adaptive neuro fuzzy inference system and support vector machine for forecasting river flow in the semiarid mountain region. *Journal of Hydrology*, 509(529), pp.379-386.
- Hol, J. (2011) *Sensor Fusion and Calibration of Inertial Sensors, Vision, Ultra-Wideband and GPS*. Department of Electrical Engineering, Linköping University, Sweden.
- Hristoforou, E. Chiria, H. Neagu, M. (1997) On the calibration of position sensors based on magnetic delay lines. *1st European magnetic sensors and actuators conference, Sensors and Actuators A: Physical*. 59,(1-3), pp. 89-93.

- Huang, P. Chen, K., Yuan, J. (2007) Motion Trajectory Planning of Space Manipulator for Joint Jerk Minimization. *International Conference on Mechatronics and Automation*, pp.3543-3548, China.
- Huang, P. Xu, Y. Liang, B. (2006) Global minimum-jerk trajectory planning of space manipulator. *International Journal of Control, Automation, and Systems*, 4(4) pp. 405-413.
- Jang, J. (1993) ANFIS: adaptive-network-based fuzzy inference systems. *IEEE Transactions on Systems, Man, and Cybernetics*, 23(3), pp. 665 - 685.
- Jang, J. (1996) Input selection for ANFIS learning. *IEEE International Conference on Fuzzy Systems*, 2, pp.1493-1499.
- Jiménez, A. Al-Hadithi, B. (2011) New methods for the estimation of Takagi – Sugeno model based extended Kalman filter and its applications to optimal control for nonlinear systems. In: *Fuzzy Control. Theory Appl*, pp. 91 – 110.
- Kaminski, M. Szermer, M. Kowalska, K. (2007) Modeling of the EMC signal disturbing sources, *CADSM ' 2007*, Ukraine.
- Kim, S. Kim, J. H. (1996) Optimal trajectory planning of a redundant manipulator using evolutionary programming. *IEEE International Conference on Evolutionary Computation*, pp738-743, Japan.
- Kovac, N. Bauk, S. (2006) The Anfis based route preference estimation in sea navigation, *Journal of Maritime Research Jmr*, 3, pp.69-86.
- Lima, F. Kaiser, W. (2010) Speed neuro-fuzzy estimator for sensorless indirect flux oriented induction motor drive. *Conference of the IEEE Industrial Electronics Society*, 2926-2931.
- Liu, H., Lai, X. (2013) Time-optimal and jerk continuous trajectory planning for robot manipulators with kinematic constraints. *Robotics and Computer-Integrated Manufacturing*, 29(2), pp. 309-317.
- Moon, J. Chang, J. Kim, S. (2013) Determining Adaptability Performance of Artificial Neuro Network-Based Thermal Control Logics for Envelope Conditions in Residential Buildings. *Energies*, 2013, 6(7), pp.3548-3570.
- Murcutt, P. D., Collins, S., & Allan, P. (2011) High level integration of remote handling control systems at JET. *Fusion Engineering and Design*. 86(9–11), pp.1911–1914.
- Nayak, P. Sudheer, K. Rangan, D. (2004) A neuro-fuzzy computing technique for modeling hydrological time series. *Journal of Hydrology*, 291(1-2), pp.52-66.

- Pan, H. (2017) *Research on Compliance Control System of Remote Handling Robot for Graphite Tile of EAST PFC*, University of Science and Technology of China.
- Peng, X. B., Song, Y. T. (2000) Conceptual design of EAST flexible in-vessel inspection system. *Fusion Engineering and Design*, 85(7–9), pp. 1362–1365.
- Shi, S. (2017) *Development of the EAST articulated maintenance arm and an algorithm study of deflection prediction and error compensation*. Lappeenranta University of Technology, School of Energy Systems, Mechanical Engineering
- Shi, S., Song, Y., Cheng, Y., Villedieu, E., Bruno, V. (2016) Conceptual design main progress of EAST Articulated Maintenance Arm (EAMA) system. *Fusion Engineering and Design*, 104, pp.40–45.
- Tada, E. Maisonnier, D. (1995) Remote handling technology development for fusion experimental reactors. *Fusion Engineering and Design*, 29, pp. 249-261.
- Thomas, A., Pattabiraman, K. (2016). Error Detector Placement for Soft Computing Applications. ACM.
- Virgala, I. Gmitterko, A. Surovec, R. (2012) Manipulator End-Effector Position Control. *Procedia Engineering*, 48, pp. 684-692.
- Wang, H., Xu, L., Chen, W. (2016) Design and implementation of visual inspection system handed in tokamak flexible in-vessel robot. *Fusion Engineering and Design*, 106, pp. 21–28.
- Wang, L., Zhang, Y., Hu, Q. S. (2008) Design and construction of vacuum control system on EAST. *Fusion Engineering and Design*, 83(2-3), pp. 295–299.
- Wei, J., Song, Y., Pei, K., Zhao, W., Zhang, Y. (2015) Conceptual design of Blanket Remote Handling System for CFETR. *Fusion Engineering and Design*, 100, pp.190–197.
- Witczak, M. (2007). *Modelling and Estimation Strategies for Fault Diagnosis of Non-Linear Systems: From Analytical to Soft Computing Approaches*. Springer Berlin Heidelberg.
- Yang, Y., Song, Y., Pan, H., Cheng, Y., Feng, H. (2016) Visual servo simulation of EAST articulated maintenance arm robot. *Fusion Engineering and Design*, 104, pp.28–33.
- Yue, S. Henrich, D. (2001) Trajectory planning in joint space for flexible robots with kinematics redundancy. *The IASTED International Conference on modeling, identification, and control*, Austria, .

Zhang, L. Slaets, P. Bruyninckx, H. (2014) An open embedded industrial robot hardware and software architecture applied to position control and visual servoing application. *Int. J. Mechatron. Autom*, pp.463 - 72.

Zhuang, Y., & Huang, H. (2014) Time-optimal trajectory planning for underactuated spacecraft using a hybrid particle swarm optimization algorithm. *Acta Astronautica*, 94(2), 690-698.

Appendix A: Data sheet of ADIS16209 and AS5047D



High Accuracy, Dual-Axis Digital Inclinometer and Accelerometer

Data Sheet

ADIS16209

FEATURES

- Dual-mode inclinometer system
 - Dual-axis, horizontal operation, $\pm 90^\circ$
 - Single-axis, vertical operation, $\pm 180^\circ$
- High accuracy, 0.1°
- Digital inclination data, 0.025° resolution
- Digital acceleration data, 0.244 mg resolution
- $\pm 1.7 \text{ g}$ accelerometer measurement range
- Digital temperature sensor output
- Digitally controlled bias calibration
- Digitally controlled sample rate
- Digitally controlled frequency response
- Dual alarm settings with rate/threshold limits
- Auxiliary digital I/O
- Digitally activated self-test
- Digitally activated low power mode
- SPI-compatible serial interface
- Auxiliary 12-bit ADC input and DAC output
- Single-supply operation: 3.0 V to 3.6 V
- 3500 g powered shock survivability

APPLICATIONS

- Platform control, stabilization, and alignment
- Tilt sensing, inclinometers, leveling
- Motion/position measurement
- Monitor/alarm devices (security, medical, safety)
- Navigation

GENERAL DESCRIPTION

The ADIS16209 is a high accuracy, digital inclinometer that accommodates both single-axis ($\pm 180^\circ$) and dual-axis ($\pm 90^\circ$) operation. The standard supply voltage (3.3 V) and serial peripheral interface (SPI) enable simple integration into most industrial system designs. A simple internal register structure handles all output data and configuration features. This includes access to the following output data: calibrated acceleration, accurate incline angles, power supply, internal temperature, auxiliary analog and digital input signals, diagnostic error flags, and programmable alarm conditions.

FUNCTIONAL BLOCK DIAGRAM

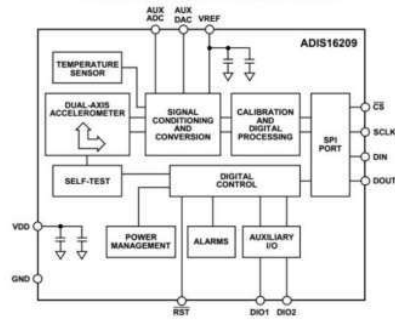


Figure 1.

Configurable operating parameters include sample rate, power management, digital filtering, auxiliary analog and digital output, offset/null adjustment, and self-test for sensor mechanical structure.

The ADIS16209 is available in a $9.2 \text{ mm} \times 9.2 \text{ mm} \times 3.9 \text{ mm}$ LGA package that operates over a temperature range of -40°C to $+125^\circ\text{C}$. It can be attached using standard RoHS-compliant solder reflow processes.

Rev. F [Document Feedback](#)
 Information furnished by Analog Devices is believed to be accurate and reliable. However, no responsibility is assumed by Analog Devices for its use, nor for any infringements of patents or other rights of third parties that may result from its use. Specifications subject to change without notice. No license is granted by implication or otherwise under any patent or patent rights of Analog Devices. Trademarks and registered trademarks are the property of their respective owners.

One Technology Way, P.O. Box 9106, Norwood, MA 02062-9106, U.S.A.
 Tel: 781.329.4700 ©2008–2017 Analog Devices, Inc. All rights reserved.
[Technical Support](#) www.analog.com



AS5047D

14-Bit On-Axis Magnetic Rotary Position Sensor with 11-Bit Decimal and Binary Incremental Pulse Count

General Description

The AS5047D is a high-resolution rotary position sensor for fast absolute angle measurement over a full 360-degree range. This new position sensor is equipped with revolutionary integrated dynamic angle error compensation (DAEC™) with almost 0 latency and offers a robust design that suppresses the influence of any homogenous external stray magnetic field.

A standard 4-wire SPI serial interface allows a host microcontroller to read 14-bit absolute angle position data from the AS5047D and to program non-volatile settings without a dedicated programmer.

Incremental movements are indicated on a set of ABI signals with a maximum resolution of 2000 steps / 500 pulses per revolution in decimal mode and 2048 steps / 512 pulses per revolution in binary mode. The resolution of the ABI signal is programmable and can be reduced to 32 steps per revolution, or 8 pulses per revolution.

Brushless DC (BLDC) motors are controlled through a standard UVW commutation interface with a programmable number of pole pairs from 1 to 7. The absolute angle position is also provided as PWM-encoded output signal.

The AS5047D is available as a single die in a compact 14-pin TSSOP package.

Ordering Information and Content Guide appear at end of datasheet.

Key Benefits & Features

The benefits and features of AS5047D, 14-Bit On-Axis Magnetic Rotary Position Sensor with 11-Bit Decimal and Binary Incremental Pulse Count are listed below:

Figure 1:
Added Value of Using the AS5047D

Benefits	Features
<ul style="list-style-type: none">• Easy to use – saving costs on DSP	<ul style="list-style-type: none">• DAEC™ Dynamic angle error compensation
<ul style="list-style-type: none">• Good resolution for motor and position control	<ul style="list-style-type: none">• 14-bit core resolution
<ul style="list-style-type: none">• Simple optical encoder replacement	<ul style="list-style-type: none">• ABI programmable decimal and binary pulse-count: 500, 400, 300, 200, 100, 50, 25, 8, 512, 256 ppr
<ul style="list-style-type: none">• No programmer needed (via SPI command)	<ul style="list-style-type: none">• Zero position, configuration programmable

Publication I

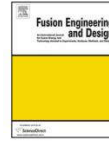
Jing, W., Huapeng, W., and Yuntao, S.
**Genetic algorithm trajectory plan optimization for EAMA: EAST Articulated
Maintenance Arm**

Reprinted with permission from
Fusion Engineering and Design
Vol. 109-111, pp. 700-706, 2016
© 2016, Elsevier



Contents lists available at ScienceDirect

Fusion Engineering and Design

journal homepage: www.elsevier.com/locate/fusengdes

Genetic algorithm trajectory plan optimization for EAMA: EAST Articulated Maintenance Arm



Jing Wu^{a,b,*}, Huapeng Wu^b, Yuntao Song^a, Yong Cheng^a, Wenglong Zhao^a, Yongbo Wang^b

^a Institute of Plasma Physics, Chinese Academy of Sciences, 350 Shushanhu Rd., Hefei, Anhui, China

^b Lappeenranta University of Technology, Skinnarilankatu 34, Lappeenranta, Finland

HIGHLIGHTS

- A redundant 10-DOF serial-articulated robot for EAST assembly and maintains is presented.
- A trajectory optimization algorithm of the robot is developed.
- A minimum jerk objective is presented to suppress machining vibration of the robot.

ARTICLE INFO

Article history:

Received 21 August 2015

Received in revised form 28 January 2016

Accepted 3 February 2016

Available online 2 March 2016

Keywords:

EAMA

Genetic algorithm

Minimum jerk

Interpolation polynomial

Trajectory planning

ABSTRACT

EAMA (EAST Articulated Maintenance Arm) is an articulated serial manipulator with 7 degrees of freedom (DOF) articulated arm followed by 3-DOF gripper, total length is 8.867 m, works in experimental advanced superconductor tokamak (EAST) vacuum vessel (VV) to perform blanket inspection and remote maintenance tasks. This paper presents a trajectory optimization method which aims to pursue the 7-DOF articulated arm a stable movement, which keeps the mounted inspection camera anti-vibration. Based on dynamics analysis, trajectory optimization algorithm adopts multi-order polynomial interpolation in joint space and high order geometry Jacobian transform. The object of optimization algorithm is to suppress end-effector movement vibration by minimizing jerk RMS (root mean square) value. The proposed solution has such characteristics which can satisfy kinematic constraints of EAMA's motion and ensure the arm running under the absolute values of velocity, acceleration and jerk boundaries. GA (genetic algorithm) is employed to find global and robust solution for this problem.

© 2016 Elsevier B.V. All rights reserved.

1. Introduction

The EAST Articulated Maintenance Arm (EAMA) is a length of 8.867 m articulated flexible robotic arm which is designed for working in the experimental advanced superconductor tokamak vacuum vessel (VV). EAMA maintenance services include a geometrically enclosed space inspection task and a graphite tile friction cleaning task for the Plasma Facing Components (PFCs) of the EAST vessel, as shown in Fig. 1.

EAMA should be able to work repetitively in a ring pattern environment through one port of the EAST vessel. To fulfill the tasks a multi-degree mechanism is designed for EAMA which composed of 7-DOF (degree-of-freedom) arm, followed by 3-DOF gripper. As the parameters shown in Fig. 2, EAMA has a light weight, redundant

and flexible structure, which brings more load capacity and operation speed. However, if the applied acceleration is discontinuous, then it may also result in a significant end-effector vibration, trajectory tracking inaccuracy and control error. In this case we could like to prohibit vibration by adjusting robot motion control.

From definition point of view, trajectory planning can be defined as to fulfill a certain motion along a given geometric path with some predefined demands, whose ultimate aim is to generate proper clue and suitable reference inputs for the control system of a robot. In practical applications, trajectory planning of motion control could reduce vibration by preventing discontinuous acceleration profile or a jerk. For instance, in Cartesian space setting minimum weighted sum of the integral squared jerk [1,2], jerk value restricted by adjusting motion parameters variance [3,4] have been applied to improve the practical performance. In joint space, preventing abrupt change of the torque to smooth angular jerk [5] or minimizing the maximum jerk in global of view [6] are adopted.

This paper presents the use of joint space trajectory planning to optimize trajectory root mean square value of jerk in Carte-

* Corresponding author at: Lappeenranta University of Technology, Skinnarilankatu 34, Lappeenranta, Finland.
E-mail address: wujing@lpp.ac.cn (J. Wu).

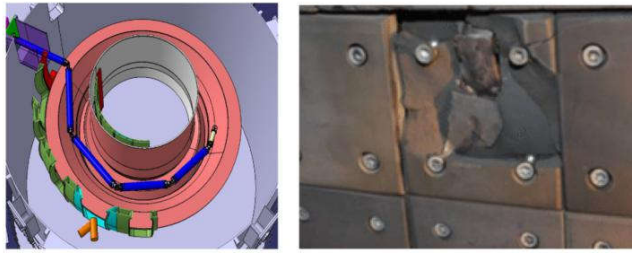


Fig. 1. EAMA in EAST vessel and graphite tile.

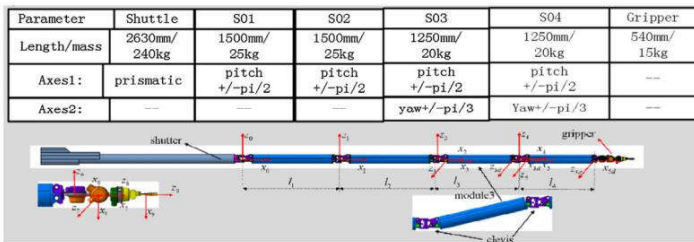


Fig. 2. Characteristics and parameters of EAMA.

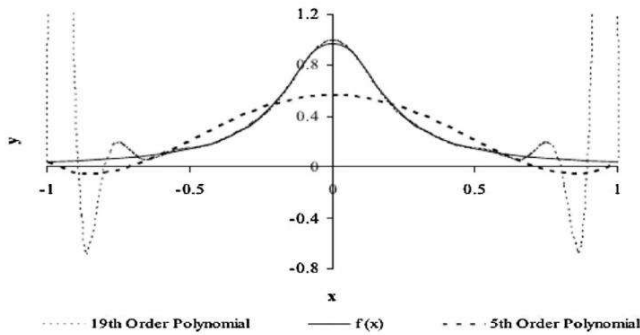


Fig. 3. Different order of polynomial interpolation.

sian space. The proposed method is based on the genetic algorithm (GA) which adopting high order geometrical Jacobian. The optimal motion of the end-effector is the one that minimizes the objectives to reduce vibration through movement. Following this introduction, the rest of the paper is organized as follows: Section 2 formulates the target problem analysis. Sections 3 and 4 present algorithm strategy, objectives and results. Finally, the last section outlines the main conclusions.

2. Target problem analysis

Due to the redundant and cantilever structure of EAMA, Cartesian trajectory planning is a very difficult task. Firstly, the trajectory performance, to a large extent, is dependent on the inverse kinematics of the arm, but the high redundant structure of the arm makes inverse kinematics more complex. Secondly, the long flexible structure may result in a more imprecise disturbance. Consider

these issues, joint space trajectory plan has significant advantage to overcome singularity problem, optimization objective makes sure the end-effector is always the controlled in minimum jerk to reduce imprecise even it has most distance from the base.

2.1. Kinematics and geometry Jacobian of EAMA

Redundant structure may lead to many difficulties in solving singularity problems [7]. Some research work, such as in literature [6,8], have been focused on this issue in joint space by taking into account the flexible robots with kinematics redundancy.

Considering the redundant and flexible structure of EAMA, the functional relationship of joint velocity with respect to task space velocity can be given as:

$$\dot{x} = J\dot{q} \tag{1}$$

where $\dot{x} = [\dot{p}_e^T \ \dot{\omega}_e^T]^T$ is a 6-dimensional vector represents end-effector velocity and angular velocity; $J = [J_p \ J_\omega]^T$ is $6 \times n$ Jacobian matrix of the forward kinematic mapping joint velocities to end-effector contribution, it is a function of joint angle; $\dot{q} = [\dot{q}_1, \dot{q}_2, \dots, \dot{q}_n]^T$ the vector of joint velocities.

$$\begin{aligned} \dot{p}_e &= J_p(q)\dot{q} \\ \dot{\omega}_e &= J_\omega(q)\dot{q} \end{aligned} \tag{2}$$

By taking derivative of the end-effector velocity and acceleration, we can obtain the end-effector jerk as:

$$\ddot{x} = \ddot{J}\dot{q} + 2\dot{J}\ddot{q} + J\ddot{\ddot{q}} \tag{3}$$

$$J = \begin{bmatrix} e_1 \times a_{1,e} \cdots e_n \times a_{n,e} \\ e_1 \cdots e_n \end{bmatrix} \tag{4}$$

In Eq. (4), e_i is unit vector parallel to revolute joint, $a_{i,j}$ is vector between i and j link origins [9].

For i th column of J , we have:

$$\dot{j}_i = \begin{bmatrix} \dot{e}_i \times a_{i,e} + e_i \times \dot{a}_{i,e} \\ \dot{e}_i \end{bmatrix} \tag{5}$$

$$\ddot{j}_i = \begin{bmatrix} \ddot{e}_i \times a_{i,e} + 2\dot{e}_i \times \dot{a}_{i,e} + e_i \times \ddot{a}_{i,e} \\ \ddot{e}_i \end{bmatrix} \tag{6}$$

2.2. Dynamic model of EAMA

Without considering joint flexibility, the optimization of Eq. (4) is subject to the following EAMA dynamics:

$$M(q)\ddot{q} + \dot{q}^T C(q)\dot{q} + G(q) = T \tag{7}$$

where T is actuator torques or force, M is mass matrix, and the C is Coriolis and centrifugal force matrix, which is linear in \dot{q} , and G is gravity force vector.

Since actuator torque rates can represent the bounded controls, the third-order dynamics is needed. Taking derivative of Eq. (7) with respect to time gives the required dynamics of the system.

$$\begin{aligned} M(q)\ddot{\ddot{q}} + \dot{M}(q)\ddot{q} + \dot{q}^T C(q)\dot{q} - \dot{q}\dot{C}(q)\dot{q} + \dot{q}^T \dot{C}(q)\dot{q} + \dot{G}(q) \\ = \dot{T} \end{aligned} \tag{8}$$

where the torque rates \dot{T} can represent the n -dimensional bounded controls.

2.3. Constraints of EAMA

(1) The boundary conditions of the initial and final position, velocity and acceleration can be written as:

$$\begin{aligned} q_0 = s_0, \dot{q}_0 = v_0, \ddot{q}_0 = a_0, \\ q_t = s_t, \dot{q}_t = v_t, \ddot{q}_t = a_t \end{aligned} \tag{9}$$

(2) The kinematic constraints related to the restriction of the maximum and minimum kinematic values of position, velocity and acceleration can be expressed as:

$$\begin{aligned} s_{\min} \leq q \leq s_{\max}, \\ v_{\min} \leq \dot{q} \leq v_{\max}, \\ a_{\min} \leq \ddot{q} \leq a_{\max} \end{aligned} \tag{10}$$

(3) Dynamic constraints with respect to torque and torque rates can be written as:

$$T_{\min} \leq T \leq T_{\max}, \tag{11}$$

$$\dot{T}_{\min} \leq \dot{T} \leq \dot{T}_{\max}$$

(4) Time constraints can be given as:

$$t_{\min} < t < t_{\max} \tag{12}$$

3. Algorithm strategy

3.1. Polynomial interpolation

After a set of knots are designed in joint space, interpolation can be done in two main ways to approach blend segments: parametric evaluation (blend from A to B over the course of several frames); numerical integration (blend one step forward from current point to tended point) [10]. For off-line model with inter knots, it is more convinced to use parametric evaluation method.

Since jerk is the derivative of acceleration, the polynomial which can represent our desired parameters should at least have forth order. But a higher order polynomial interpolation is not recommended because of the local smoothness and coefficient solution problems [11], as demonstrated in Fig. 3.

EAST application requires inspection stability for entire trip, so inter knots demand jerk limitation as well. Assuming we have k knots, except for the initial and end points, we still have $k-2$ inter knots. For each smooth inter knot, the end velocity and position of inter knot i should be equal to the start velocity and position of inter knot $i+1$. The trajectory equations are as follows:

$$q_{i,i+1} = c_{i0} + c_{i1}t + c_{i2}t^2 + c_{i3}t^3 + c_{i4}t^4 + c_{i5}t^5 \tag{13}$$

where c_i is coefficient of polynomial interpolation satisfied from inter knot i to $i+1$ during time t . Differentiate this equation yields:

$$\begin{aligned} \dot{q}_{i,i+1}(t) &= c_{i1} + 2c_{i2}t + 3c_{i3}t^2 + 4c_{i4}t^3 + 5c_{i5}t^4 \\ \ddot{q}_{i,i+1}(t) &= 2c_{i2} + 6c_{i3}t + 12c_{i4}t^2 + 20c_{i5}t^3 \\ \ddot{\ddot{q}}_{i,i+1}(t) &= 6c_{i3} + 24c_{i4}t + 60c_{i5}t^2 \\ c_{i0} &= q_i \\ c_{i1} &= \dot{q}_i \\ c_{i2} &= \frac{\ddot{q}_i}{2} \\ \text{iff } i < k-1 \\ c_{i3} &= \frac{(4q_{i+1} - \dot{q}_{i+1}T_i - 4q_i - 3\dot{q}_i T_i - \ddot{q}_i T_i^2)}{T_i^3} \\ c_{i4} &= \frac{(\dot{q}_{i+1}T - 3q_{i+1} + 3q_i + 2\dot{q}_i T_i - \ddot{q}_i T_i^2/2)}{T_i^4} \\ &\text{else} \\ c_{i3} &= \frac{(20q_{i+1} - 8\dot{q}_{i+1}T_i - 20q_i - 12\dot{q}_i T_i - 3\ddot{q}_i T_i^2 + \dot{q}_{i+1}T_i^2)}{2T_i^3} \\ c_{i4} &= \frac{(-30q_{i+1} + 14\dot{q}_{i+1}T_i + 30q_i + 16\dot{q}_i T_i + 3\ddot{q}_i T_i^2 - 2\dot{q}_{i+1}T_i^2)}{2T_i^4} \\ c_{i5} &= \frac{(12\dot{q}_{i+1} - 6\dot{q}_{i+1}T_i - 12q_i - 6\dot{q}_i T_i - \ddot{q}_i T_i^2 + \dot{q}_{i+1}T_i^2)}{2T_i^5} \end{aligned} \tag{14}$$

If $i < k-1$, then c_{i5} is equal to 0 in Eq. (13), the coefficient can be obtained by any given position, velocity and acceleration. T_i is running time between knots i and $i+1$. Furthermore, the end-effector jerk of x_{i+1} can be calculated by Eq. (3). Therefore, the relationship

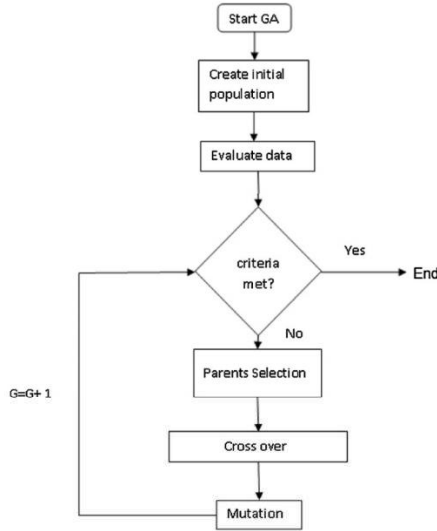


Fig. 4. Genetic algorithm optimization procedure.

between end-effector jerk and joint velocity, acceleration, as well as the joint jerk can be expressed by time and other parameters. The objective function becomes to minimize the root mean square of end-effector jerk [12]:

$$\begin{aligned} \text{Min: } \sum \text{jerk}_{rms} &= \sum \sqrt{\left| \frac{1}{t_k - t_0} \int_{t_0}^{t_k} \ddot{x}(q, \dot{q}, \ddot{q}, t) dt \right|^2} \\ &= \sum \sqrt{\left| \frac{\dot{x}(t_k) - \dot{x}(t_0)}{t_k - t_0} \right|^2} \end{aligned} \quad (15)$$

3.2. GA for RMS jerk of EAMA

To find the best parameters that satisfy the minimum jerk, the genetic algorithm (GA) is applied. As shown in Fig. 4, GA is a population-based stochastic and global search method, imitates the natural biological evolution process [13]. First, it starts on generating a population of individuals. Then this population comes to an evolutionary process, which passes individuals to objective function. After that, it undergoes a loop searching criteria, which contains selection, crossover and mutation, and the better individuals will have more possibilities to reproduce the next generations. The detailed procedure is listed in Table 1 as pseudo code.

4. Simulation work and result

In order to verify the performance of our algorithm and the theoretical hypothesis, a point to point movement simulation was performed in this work.

The evolution movement simulation was carried out by the three segments which try to turn right from initial position as shown in Table 2, while the other two segments are kept stillness. In the joint space evolution, we assume the links start initial statement and finish at the end statement. Bound restriction for angle, velocity, acceleration are listed. Meanwhile, suppose we have a unit

Table 1
GA for RMS jerk Pseudo code.

```

GA for RMS jerk
-----
Begin
t: = 0;
lb: = lower bound for restriction;
ub: = upper bound for restriction;
pt: = a population of n randomly-generated individuals;
e: = solution from settled min-jerk;
while pt < lb or pt > ub or not solution found do
Create the initial population p0;
Evaluate the initial population;
while not solution found or termination-condition do
t: = t + 1;
Create generation t + 1;
1. Copy:
Select (1 - c) × n members of pt and insert into pt+1;
2. Crossover:
Select χ × n members of pt; pair them up; produce offspring; insert the offspring into pt+1;
3. Mutate:
Select μ × n members of pt+1; invert a randomly-selected bit in each;
Reproduce select individuals
Evaluate pt+1;
od
if solution found exist;
od
end
    
```

Note: when p_t is within the bounds, initial population p₀ is created, scores each member of the p₀, if the termination-condition is not met by current population, then start the loop to create next generation, children are produced either by making random changes to a single parent or by combining the vector entries of a pair of parents. Replace the current population with the children, repeat this loop until solution is found. Where n is the number of individuals in the population; χ is the fraction of the population to be replaced by crossover in each iteration; and μ is the mutation rate. From Eq. (15), we have a function $\bar{x} = f(q, \dot{q}, \ddot{q}, t)$, which we want to optimize.

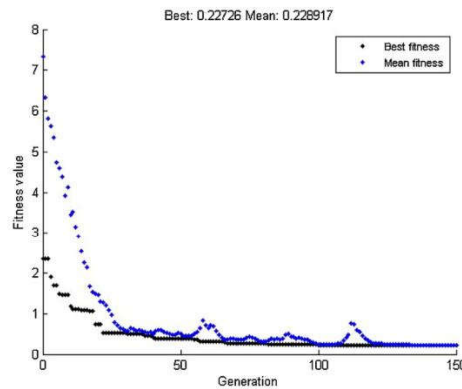


Fig. 5. Minimum jerk of end-effector deformation versus number of generations.

time constant for each travel of inter-knot as well as an intermediate via point, then we can employ the GA algorithm to search for the best inter-knot point under the given constraint conditions. The aim is to minimize the objective function to find a set of optimal joint angles and angular velocity values for the inter-knot points. To simplify the complicated computation, 150 generations are applied due to tiny changing rate after a certain amount of generation passed. According to the simulation result in Fig. 5, it can be seen that both of the average value and best fitness value of the GA optimization

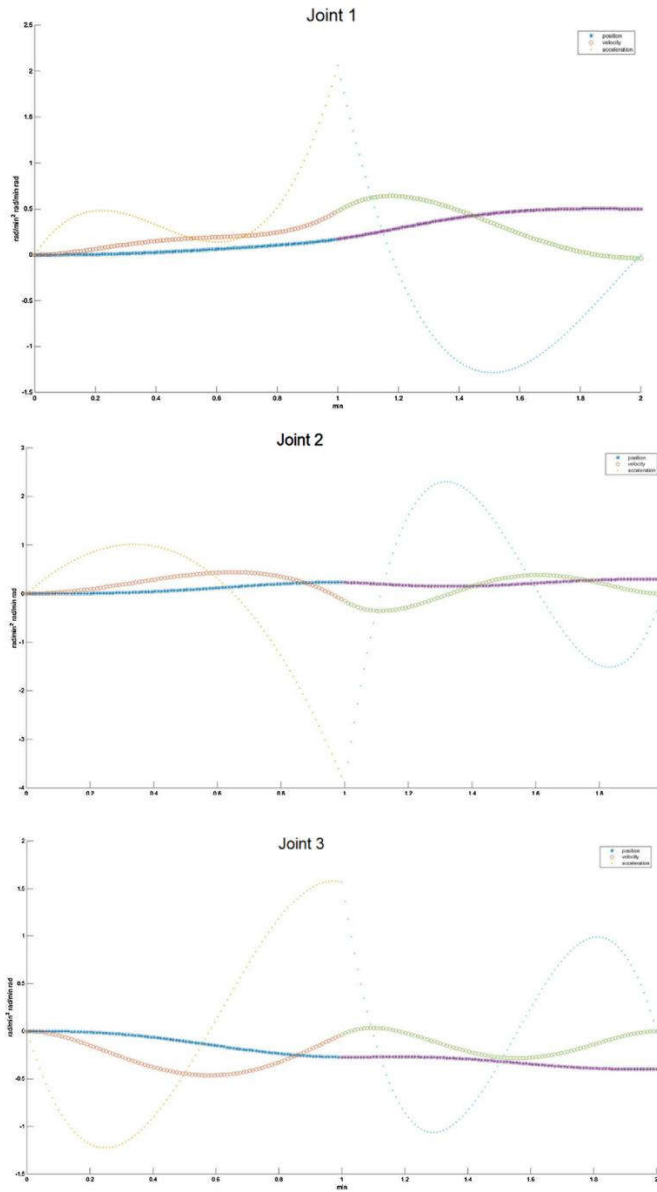


Fig. 6. Trajectory result for joint 1–3.

objective function decrease rapidly at the beginning, but after 50 generations it approaches to a comparing steady value.

After 150 generations, the convergent solution value for best fitness of the objective function (14) is 0.22726 and the average

value is 0.228917. For the best fitness case, the middle joints angle, velocity and acceleration of the three links are listed in Table 2, and the joint position trajectory of joints 1, 2 and 3 are illustrated in Fig. 6.

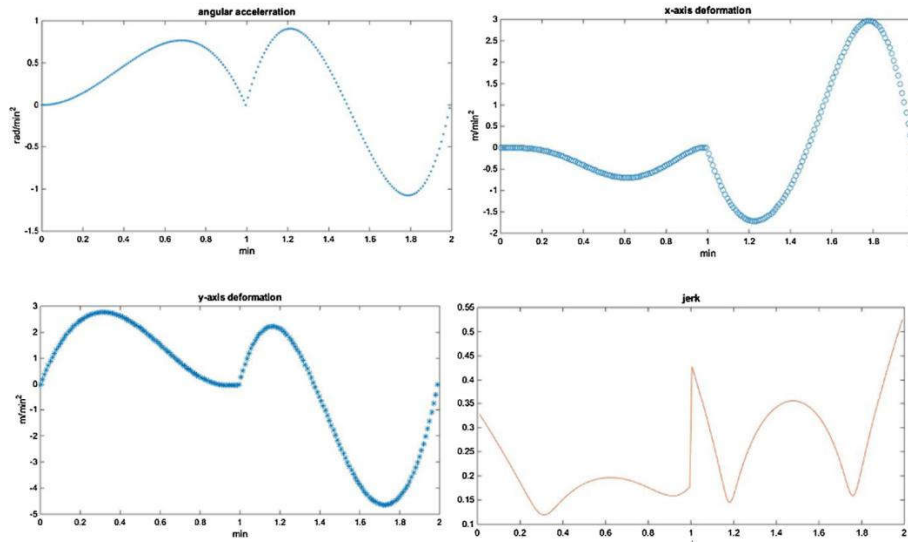


Fig. 7. Trajectory result for end-effector on angular acceleration, liner deformation on x, y-axis linear acceleration and jerk result.

Table 2
Parameters and middle point from GA of RMS result.

GA parameter Experiment result	Population number: 50 Angle (rad)	Cross over rate: 0.8 Velocity (rad/min)	Mutation rate: constraint dependent Acceleration (rad/min^2)
Joint 1			
Initial	0	0	0
Middle	0.171	0.477	2.06
End	0.5	0	0
Joint 2			
Initial	0	0	0
Middle	0.231	-0.151	-3.921
End	0.3	0	0
Joint 3			
Initial	0	0	0
Middle	-0.272	-0.035	1.569
End	-0.4	0	0
Lower and upper boundaries	[0 rad 0 rad -0.4 rad; 0.5 rad 0.3 rad 0 rad]	[±1 rad/min]	[±4 rad/min ²]

Fig. 7 gives the detailed motion changing of end-effector movement, comparing with previous research [6], end-effector jerk value is targeted and limited. Meanwhile, even though we have one more joint been invited into the optimization, the convergent speed is much faster and final optimal value is smaller than in reference [6] (50 generations vs 300 generations), this is due to the different the numbers of population; different rates of crossover and mutation are chose. From the joint trajectory side in Fig. 6 each joint can satisfy constraints requirement. It is possible to exam the algorithm with more or less segments. We also simulated the point to point movement with two links, when more DOFs added only the computation cost will be increased. However, from global view all the joints should be tested not only in some special important motion, such that the end-effector jerk value in full motion can be obtained. By adding more inter knots and optimization parameter vectors, GA of RMS could work in a more complicated situation or even com-

bine with more optimization goal such as moving time or energy [14].

5. Conclusion

Finally, in this paper, we developed an algorithm to minimize the end-effector jerk movement for a multi-DOF manipulator EAMA. It provide optimal ability by adopting genetic algorithm to find root mean square value of jerk for desired movement. The results of the optimized trajectory not only be used for model based dynamic control, but can also be used for offering good resource for robot vision and the further research subjects. More research work will be carried out in the future to minimize the disturbance and to enhance stability of EAMA in other related works such as control scheme planning, software design and hardware design. Develop-

ment of EAMA may also lead to a different type of EAST maintenance and repair service.

Acknowledgments

This project is supported by Chinese ITER Special Support Project, No. 2014GB101000. We deeply thank to colleagues of Lappeenranta University of Technology for their hard work and beneficial discussions.

References

- [1] A. Gasparetto, V. Zanotto, Optimal trajectory planning for industrial robots, *Adv. Eng. Softw.* 41 (4) (2010) 548–556.
- [2] A. Gasparetto, V. Zanotto, A new method for smooth trajectory planning of robot manipulators, *Mech. Mach. Theory* 42 (4) (2007) 455–471.
- [3] H. Liu, X. Lai, W. Wu, Time-optimal and jerk continuous trajectory planning for robot manipulators with kinematic constraints, *Rob. Comput. Integr. Manuf.* 29 (2) (2013) 309–317.
- [4] R. Bearsee, A. Olabi, Dissociated jerk-limited trajectory applied to time-varying vibration reduction, *Rob. Comput. Integr. Manuf.* 29 (2) (2013) 444–453.
- [5] D. Constantinescu, E.A. Croft, Smooth and time-optimal trajectory planning for industrial manipulators along specified paths, *J. Rob. Syst.* 17 (5) (2000) 233–249.
- [6] Y. Huang, Global minimum-jerk trajectory planning of space manipulator, *Int. J. Control Autom. Syst.* 4 (4) (2006) 405–413.
- [7] S. Kim, J.H. Kim, Optimal trajectory planning of a redundant manipulator using evolutionary programming, in: *IEEE International Conference on Evolutionary Computation*, May, 1996, pp. 738–743.
- [8] D. Yue, W. Henrich, Trajectory planning in joint space for flexible robots with kinematics redundancy, in: *The IASTED International Conference on Modeling, Identification, and Control*, February 19–22, Innsbruck, Austria, 2001.
- [9] P. Freeman, Minimum Jerk Trajectory Planning for Trajectory Constrained Redundant Robots, *Electronic Theses and Dissertations*, 2012.
- [10] M. Acton, et al., *Math for Game Programmers*, Sessions at GDC Game Developers Conference, March, 2012.
- [11] Y. Guan, K. Yokoi, O. Stasse, A. Kheddar, On robotic trajectory planning using polynomial interpolations, *IEEE Transl. J. Rob. Biomim.* (2005) 111–116.
- [12] S. K. Saha, in: *Introduction to Robotics*, McGraw Hill Education (India) Private Limited, 2008.
- [13] D. Vose Michael, *The Simple Genetic Algorithm: Foundations and Theory*, MIT Press, 1999.
- [14] S. Števo, I. Sekaj, Optimization of robotic arm trajectory using genetic algorithm, in: *19th World Congress the International Federation of Automatic Control Cape Town, South Africa*, August 24–29, 2016, p. 201.

Publication II

**Extended Kalman filter estimator with curve fitting calibration of EAST
Articulated Maintenance Arm position disturbance compensation**

Reprinted with permission from
Jing, W., Yuntao, S., and Huapeng, W.
*Electronic Information and Communication Technology (ICEICT), 2016 IEEE
International Conference on
March/2017*
© 2017, IEEE

Extended Kalman Filter Estimator with Curve Fitting Calibration of EAST Articulated Maintenance Arm Position Disturbance Compensation

Jing Wu^{1,2}, Yuntao Song, Yu Han, Songzhu Yang
Institute of Plasma Physics Chinese Academy of Sciences,
350 Shushanhu Road Hefei Anhui, China
Email:wujing@ipp.ac.cn

Huapeng Wu, Wenlong Zhao
Lappeenranta University of Technology, Skinnarilankatu 34
Lappeenranta, Finland

Abstract—EAMA (EAST Articulated Maintenance Arm) is an articulated serial robot arm working in experimental advanced superconductor tokamak for inspection and maintenance. This paper implements an algorithm to calibrate the segment position compensation error and estimate its signal. First, the error model is curve fitted, which has unneglectable nonlinearities. Second, extended kalman filter is adapted to accurate the segment position compensation error value based on curve fitted model. The simulation result shows that the root mean squared error is reduced from 0.03602 degree to 0.0152 degree, provides significant result improvement, which satisfied the accuracy requirement up to 0.02 degree.

Keywords—EAMA; position sensor; curve fitting; EKF; calibration

I. INTRODUCTION

A. Background

The EAST group built a long articulated flexible robotic arm called EAMA (EAST Articulated Maintenance Arm) for the experimental advanced superconductor tokamak vacuum vessel (VV) [1]. EAMA is duty on a geometrically enclosed space inspection task and a graphite tile friction cleaning task for the Plasma Facing Components (PFCs) of the EAST vessel, as shown in Figure 1[2].

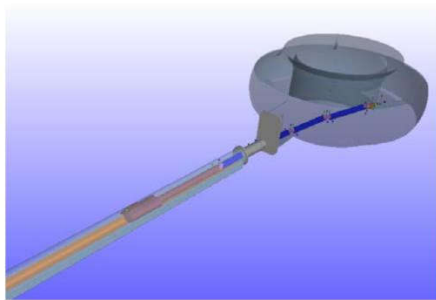


Fig. 1. EAMA in EAST vacuum vessel.

Such remotely servicing tasks using manipulators or redundant mechanisms require accurate and reliable operations with sensible result to manage their control in workspace [3].

Similar with other manipulator product, EAMA is equipped with magnetic rotary position sensor, which is an electromechanical device that converts the angular position of a shaft or axle to analog or digital code.

B. Error Resource

For most mechanism reason, we adapted AS5047D as our encoder, which is illustrated in Figure 2[4]. The chip is fixed on the bear housing and the magnet is attached to the shaft, which axis of the magnet must be aligned over the center of the package. But the gap between the inner ring and outer ring brings some sort of beatings which result in a difficulty of axis aligning when rotor is running, as shown in Figure 3. Beside the mechanical factor, the signal is also affected by EMC disturbance [5]. In summary, the patterns of sample time and error from joints are clear regular periodical.

C. Previous research

Sensor calibration usually can be archived by iterative algorithm methods [6], by the means of assistant devices compensation [7], multi-sensor fusion measurement [8] or physical adjustment [9]. It is noticed that filtering with a proper model is more applicable for only software calibration, which is emphases in our work.

This paper presents the use of Extended Kalman Filter to estimate the compensation error from a curve fitted idealized model of the difference between reference data and experiment measurement. The proposed curve fitting method is based on the Trust-Region-Reflective Least Squares algorithm, which adopts multi-terms sum of sine waves. The optimal result of estimate error is reduced from 0.03602 degree to 0.0152 degree, of which accuracy is satisfied with 0.020 degree. Following this introduction, the rest of the paper is organized as follows: Section 2 formulates the target model analysis, curve fitting. Section 3, 4 present Extended Kalman Filter algorithm strategy, objectives and test results. Finally, the last section outlines the main conclusions.

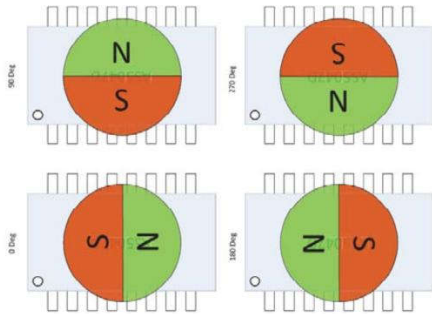


Fig. 2. Angle detection by AS5047D.

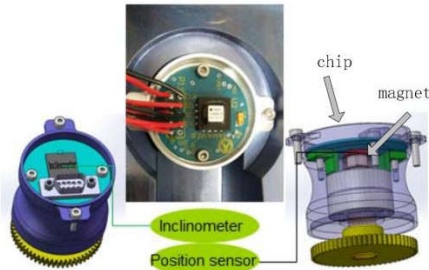


Fig. 3. Mechanical installation of AS5047D.

II. CURVE FITTING

A. Error Model Analysis

First, we install the test bench as shown in Figure 4. The motor is connected to a reducer, which is followed by a reference encoder and a demo board on the same shaft. The sample period is united for reference encoder and demo board. The rotation speed is settled to 1 degree per second, the first segment sample rate is 0.125 second, and the second segment sample rate is 0.25 second. We have the results of both segments drawn in Figure 5, which adhere to regular periodical form, and are aligned to a certain amplitude region.

B. Curve Fitting 4 Times Term Sum of Sine Coefficient

Due to the wave-like form of error, the sum of simple sine waves series function is a way to represent error model, as in

$$f(x) = \sum_{n=1}^4 (a_n * \sin(b_n * x) + C_n) \quad (1)$$

Considering that the nonlinear least squares problem can be written in the terms below [10], γ represents the sine coefficient.

$$u(\gamma) = \sum_{i=1}^m (y_i - f(x_i, \gamma))^2 \quad (2)$$

The optimization algorithm used for the least squares minimization is the Trust-Region-Reflective (TRR) [11]. It is one of the algorithms, which give more accurate and less costly results [12]. The algorithm is presented in Table 1.

Where $U(x)$ is target minimization function, g is gradient and H is Hessian, in 2 dimensional subspace vectors and they are the direction of gradient at x_i and approximate Gauss-Newton direction, Δ_k is the trust region size.

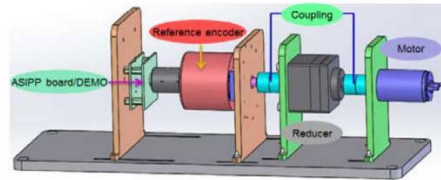


Fig. 4. Error model test bench.

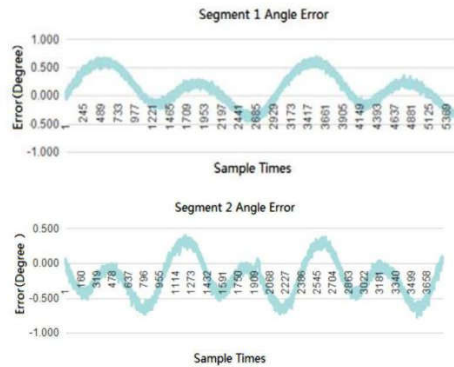


Fig. 5. Angle error of segments.

The optimized result is illustrated in Figure 6. Goodness of fit is obtained:

- The sum of squares due to error (SSE) :3.837
- R-square :0.9843
- Adjusted R-square 0.9842
- Root mean squared error (RMSE) :0.03602

TABLE I. TRUST-REGION-REFLECTIVE PSEUDO-CODE

<i>Pseudo-code of RTT</i>
Set the starting point at x_0 for $U(x_0)$,
Set the iteration number $k=1$
For $k=1, 2, \dots$
At the k -th iteration, the trial step is computed by solving trust-region sub-problem $\min \varphi_k(s_k) = g^T s_k + \frac{1}{2} s_k^T H s_k$
Evaluate s_k from equation
If $U(x_k + s_k) \leq U(x_k)$, then x_{k+1} become the current point
Else $x_{k+1} = x_k$, current point remains
Update Δ_k
If $\nabla U(s_k) \leq \text{chosen tolerance}$ then end loop
Else Continue the loop and increment k

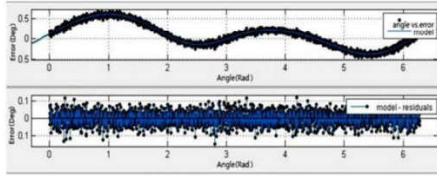


Fig. 6. Curve fitting result.

III. EXTENDED KALMAN FILTER

Extended Kalman filter (EKF)-based solutions have been investigated in many fields by the studies such as in [13] [14] for the simultaneous estimation problem. For nonlinear dynamic systems with unconstrained noise, the Kalman filter extended by system linearization of near the current parameter estimates, updates parameters consistently with all previous measurement data and converges in a few iterations generally [15]. It is rather powerful, stable and efficient for nonlinear desecrated state model.

A. Discretisation of The Error Model

The position error is modeled in the standard (degree, radian) reference frame model given as follows

$$\begin{bmatrix} error \\ angle \end{bmatrix} = \begin{bmatrix} \sum_{n=1}^d (a_n * \sin(b_n * x) + C_n) \\ angle \ step \end{bmatrix} \quad (3)$$

Before EKF application, the above model needs to be discrete in time state space [16]. Since that the input vector of the velocity is nearly constant 1 degree per second during a sampling period $T = 0.125$ second, the previous continuous model converts to the following discrete-time state space model, as in equation (4). For step k , x is the size of angle step, typically in our case it is $\pi/1500$. Equation (5) forms the EKF state model.

$$\begin{bmatrix} error_k \\ angle_k \end{bmatrix} = \begin{bmatrix} \sum_{n=1}^d (a_n * \sin(b_n * k * x) + C_n) \\ x \end{bmatrix} \quad (4)$$

$$X_k = \begin{bmatrix} \sum_{n=1}^d (a_n * \sin(b_n * k * X_{k-1}^T(2)) + C_n) \\ X_{k-1}^T(2) \end{bmatrix} \quad (5)$$

B. Classical EKF

However, most practical problems are nonlinear. The system differential equation becomes a Taylor series, and we can linearize the estimation around the current estimate by partial derivatives called a Jacobian of the process and measurement functions to compute estimates even with nonlinear relationships [17].

This approach involves math work below, which includes model establish, prediction and correction three parts: equation (6) presents model establishment, equation (7) gives the prediction of current state and equation (8) completes correction step.

$$\begin{aligned} x(k) &= f(x(k-1), u(k-1), w(k-1)) \\ z(k) &= h(x(k), v(k)) \end{aligned} \quad (6)$$

$$\begin{aligned} \tilde{x}(k) &= f(x(k-1), u(k-1), 0) \\ \tilde{z}(k) &= h(\tilde{x}(k), 0) \\ \tilde{p}(k) &= A(k) * p(k-1) * A^T(k) + \\ & W(k) * Q(k-1) * W^T(k) \end{aligned} \quad (7)$$

$$\begin{aligned} K(k) &= \tilde{p}(k) * H^T(k) * (H(k) * \tilde{p}(k) * H^T(k) + \\ & V(k) * R(k) * V^T(k))^{-1} \\ p(k) &= (I - K(k) * H(k)) * \tilde{p}(k) \\ x(k) &= \tilde{x}(k) + K(k) * (z(k) - h(\tilde{x}(k), 0)) \end{aligned} \quad (8)$$

- $x(k)$ is non-linear system stochastic difference equation.
- $z(k)$ is the measurement that is returned from the sensors at each position.
- $w(k-1)$, $v(k)$ are process and measurement noise.
- $\tilde{x}(k)$ and $\tilde{z}(k)$ approximate the state and measurement vector.
- $\tilde{p}(k)$ and $p(k)$ are priori estimate error covariance and post estimate error covariance
- K is kalman gain. This matrix gets updates as part of the measurement update stage.
- $x(k)$ is posteriori state estimate

A , H , W and V are Jacobian matrices of partial derivatives.

$$A [i,j] = \frac{\partial f[i]}{\partial x[j]}(\tilde{x}_k, u_k, 0)$$

$$W [i,j]=\frac{\partial f[i]}{\partial w[j]}(\tilde{x}_k, u_k, 0)$$

$$H [i,j]=\frac{\partial h[i]}{\partial x[j]}(\tilde{x}_k, 0)$$

$$V [i,j]=\frac{\partial h[i]}{\partial v[j]}(\tilde{x}_k, 0) \quad (9)$$

$$A_k = \begin{bmatrix} 0 & \sum_{n=1}^4 (k \cdot a_n \cdot b_n \cdot \cos(b_n \cdot k \cdot X) + C_n) \\ 0 & 1 \end{bmatrix} \quad (10)$$

Q is the covariance of the process noise. This matrix represents the uncertainty of sample stage. Even with certain rotation speed and sample time, there are still errors in each action from the time, from the commanded position issued until it actually acquire. R is measurement noise covariance, which defines the confidence of the error sensed.

IV. SIMULATION RESULT

The main objective of the simulation is to evaluate the improved accuracy of error compensation estimator, where estimated error and position are included as a part of segment of joint space control strategy. The estimator plant Matlab/Simulink® block is designed as shown in Figure 7, the embedded algorithm is described in Table II. Initialization of the system parameters: the Jacobian matrices are identity matrices and the covariance matrices are set from experiment results. Initialize the posteriori state estimate to $[1; 3\pi/500]$, which can be any value in theory. Here the chosen value is a bit off trace for a clear distinguishes. The posteriori error covariance estimate is initiated to an identity matrix.

The iteration turns 2920 times with each step $\pi/1500$ radian. The results are shown in Figure 8. The differences in position and frequency estimations between the two estimators are rather synchronous as we can see in Figure 8. Frequency represents the sample process state estimation. Position represents the error state estimation, which we could like to compensate in control strategy.

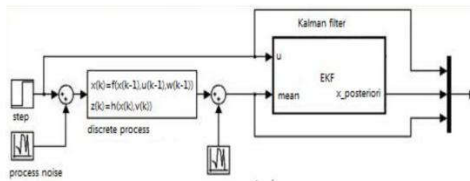


Fig. 7. Block diagram of the extended Kalman estimator.

TABLE II. TRUST-REGION-REFLECTIVE PSEUDO-CODE

Pseudo-code of EKF	
/* initialize: get system information and initial conditions */	
(Model Constants)	
State-error Jacobian	
Measurement-state Jacobian	
Measurement-error Jacobian	
(State variable initializations)	
Number of iterations	
Kalman Gain	
True initial state	
Initial posteriori state estimate	
Process noise covariance	
Measurement noise covariance	
Initial posteriori error covariance estimate	
(Iteration loop)	
For k= 2:iteration	
Update true state	
$x(k) = f(x(k-1), u(k-1), w(k-1))$	
Update measurements	
$z(k) = h(x(z), v(k))$	
Update priori estimate	
$\hat{x}(k) = \hat{x}(k-1), u(k-1), 0$	
Update state Jacobian	
$A_k = \begin{bmatrix} 0 & \sum_{n=1}^4 (k \cdot a_n \cdot b_n \cdot \cos(b_n \cdot k \cdot X) + C_n) \\ 0 & 1 \end{bmatrix}$	
knowledge of Q and R	
$Q_k = Q;$	
$R_k = R;$	
Update priori error covariance estimate	
$\hat{p}(k) = \hat{A}(k) \cdot p(k-1) \cdot \hat{A}^T + W(k) \cdot Q(k-1) \cdot W^T(k)$	
Update Kalman gain	
$K(k) = \hat{p}(k) \cdot \hat{H}^T(k) \cdot (\hat{H}(k) \cdot \hat{p}(k) \cdot \hat{H}^T(k) + V(k) \cdot R(k) \cdot V^T(k))^{-1}$	
Update posteriori state estimate	
$\hat{x}(k) = \hat{x}(k) + K(k) \cdot (z(k) - h(\hat{x}(k), 0))$	
Update posteriori error covariance estimate	
$p(k) = (I - K(k) \cdot \hat{H}(k)) \cdot \hat{p}(k)$	
end	

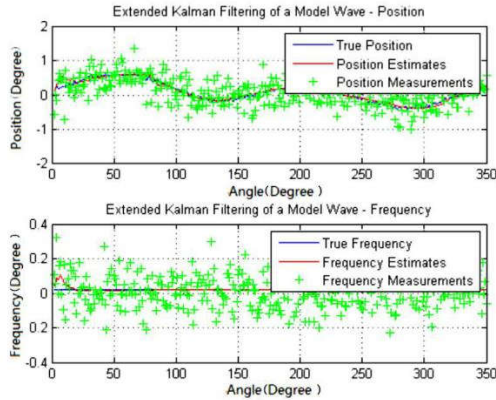


Fig. 8. Simulation result for EKF estimator.

For the first several iterations, the result shows a clear tremble. As the program running, the estimated data flow of error position and frequency turns convergence synchronously. The performances of the frequency and position tracking capabilities of EKF estimator compared to the curve fitting model based measurement has been improved about 57%, especially at this low speed. The RMSE value has been reduced from 0.03602 degree to 0.0152 degree, which now is satisfied with the control requirement of 0.02 degree.

V. CONCLUSION

Software sensor calibration is an attractive solution particularly in the case of mechanical loading factor, which doesn't have much tolerance on cost and reliability. Nevertheless the performances require the estimation of compensate position error below 0.02 degree disturbance. In this paper we have developed a data-driven modeling and robust Extended Kalman Filter optimal version estimator. Simulation results and laboratory tests (Figure 9) have demonstrated the performance, while keeping the same error tracking capabilities. This algorithm is useful in all segments to track more parameters or to implement the algorithm on top with more demonstrations than just in each joint for a cheaper or less power consumption target.



Fig. 9. laboratory test bench for EKF estimator.

ACKNOWLEDGMENT

On the completion of this paper, I should like to express my deepest gratitude to all those, whose kindness and advice have made this work possible. This project is supported by Chinese ITER Special Support Project, No. 2014GB101000. We deeply thank colleagues of Lappeenranta University of Technology for their hard work and beneficial discussions.

REFERENCES

- [1] J. Wu, H. Wu, and Y. Song, "Genetic algorithm trajectory plan optimization for EAMA: EAST Articulated Maintenance Arm", Fusion Engineering and Design, in press.
- [2] J. Wu, H. Wu, and Y. Song, "Open software architecture for east articulated maintenance arm", Fusion Engineering and Design, in press.
- [3] I. Virgala, A. Gmitterko, R. Surovec, "Manipulator End-Effector Position Control", Procedia Engineering, Volume 48, 2012, Pages 684-692
- [4] <http://ams.com/eng/Products/Magnetic-Position-Sensors/Angle-Position-On-Axis/AS5047D>
- [5] M. Kaminski, M. Szermer, K. Kowalska, "Modeling of the EMC signal disturbing sources", CADSM'2007, February 20-24, 2007, Polyana, Ukraine
- [6] E. Dorveaux, D. Vissière, A. Martin, J. Clerk Maxwell, "Iterative calibration method for inertial and magnetic sensors" 48th IEEE Conference on Decision and Control and 28th Chinese Control Conference Shanghai, P.R. China, December 16-18, 2009
- [7] <http://alliancesensors.com/linear-position-sensor-calibration-using-senset%E2%84%A2-field-programmability>
- [8] J. Hol, "Sensor Fusion and Calibration of Inertial Sensors, Vision, Ultra-Wideband and GPS", Department of Electrical Engineering, Linköping University, Sweden, 2011
- [9] E. Hristoforou, H. Chiria, M. Neagu, "On the calibration of position sensors based on magnetic delay lines". 1st European magnetic sensors and actuators conference, Sensors and Actuators A: Physical, Volume 59, Issues 1-3, April 1997, Pages 89-93
- [10] Y. Yuan, "A review of trust region algorithms for optimization." In ICIAM, Vol. 99, 2000.
- [11] Mathworks.R2012 Documentation. Optimization Toolbox- LeastSquares(ModelFitting)Algorithms. <http://www.mathworks.com/help/toolbox/optim/ug/bmoybu.html>
- [12] J. Hung, "Energy Optimization of a Diatomic System", University of Washington, Seattle, WA.
- [13] M. Barut, R. Demir, E. Zerdali, "Real-Time Implementation of Bi Input-Extended Kalman Filter-Based Estimator for Speed-Sensorless Control of Induction Motors," IEEE Transactions on Industrial Electronics, vol. 59, No. 11, November 2012
- [14] A. Akrad, M. Hilairat, D. Diallo, "A sensorless PMSM drive with a two stage extended Kalman estimator," Industrial Electronics, 2008. IECON 2008. 34th Annual Conference of IEEE
- [15] A. Jiménez, B. M. Al-Hadithi, F. Matía "Extended Kalman Filter for the Estimation and Optimal Control of Takagi-Sugeno Fuzzy Model," In: Fuzzy Control. Theory Appl, pp. 91-110 (2011)
- [16] P. Eberhard, Q. Tang, "Sensor Data Fusion for the Localization and Position Control of One Kind of Omnidirectional Mobile Robots", Multibody System Dynamics, Robotics and Control, pp 45-73, 06 November 2012
- [17] G. F. Welch and G. Bishop, "An Introduction to the Kalman Filter," University of North Carolina, Chapel Hill, NC, USA, Tech. Rep., 1995.

Publication III

**Soft computing methods compensation for EAST articulated maintenance arm
position disturbance**

Reprinted with permission from
Jing, W., Huapeng, W., and Yuntao, S.
SENSORS, 2017 IEEE, December/2017
© 2017, IEEE

Soft Computing Methods Compensation for EAST Articulated Maintenance Arm Position Disturbance

Jing Wu, Huapeng Wu, Yuntao Song, Yong Cheng
Mechanical Engineering
Lappeenranta University of Technology, Skinnarilankatu 34
Lappeenranta, Finland
Institute of Plasma Physics, Chinese Academy of Sciences
Hefei, China
wujing@ipp.ac.cn

Abstract—EAST Articulated Maintenance Arm is an articulated serial robot arm for inspection and maintenance in an experimental advanced superconductor tokamak. This paper implements soft computing algorithm for software calibration and compensation of pitch joint movement. An adaptive neuro-fuzzy inference system is applied to forecast the disclosed hysteresis loop compensation data. Joint position accuracy is significantly improved: maximum accuracy is 0.1 degree; repeatable accuracy is 0.05 degree; and RSM accuracy is 0.02 degree.

Keywords—soft computing; ANFIS; Position sensor; error compensation estimator; EAMA

I. INTRODUCTION (Heading 1)

EAMA (EAST Articulated Maintenance Arm) operates in a challenging environment of vacuum pressure (10^{-5} Pa), high temperatures ($120\text{ }^{\circ}\text{C}$) and high levels of radiation, and consequently sensors regularly need to be reassembled and reintegrated to enable routine operations. These actions introduce a specific error along with the movement, which exacerbates the propagation of uncertainty. The sensors used for position feedback of the EAMA joint should have accuracy higher than 0.14° , so that the flexible model that is built based on tests and combined with a position sensor and inclinometer can compensate the mechanical deformation. In Figure 1, each segment is equipped with an capsule containing a magnetic rotary position sensor, which is an electromechanical device that converts the angular position of a shaft or axle to digital code.

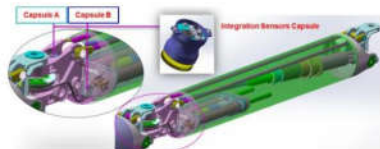


Fig. 1. EAMA segment 4 integration sensors capsule mechanism installation.

A number of approaches exist for compensation of sensing error, for example, iterative algorithm methods [1], the use of

assistant devices, such as a camera motion tracking system [2], multi-sensor fusion measurement [3] such as sensor data fusion for localization and position measurement [4], and physical adjustment [5]. The very compact construction of EAMA precludes the use of assistant devices or multi-sensor fusion. Physical adjustment could overcome offset errors, but for a high repeatability, calibration table is barely enough. In light of the above constraints, software calibration would appear the most appropriate solution of the approaches currently available. However, software calibration requires filtering with a proper model, but acquisition of the model from sensed results or deduced from all possible reasons is not straightforward. Consequently, the use of intelligent hybrid systems is growing rapidly, with successful applications available for process control, especially for model-less applications. In recent years, much research has been undertaken in the areas of senseless estimation [6], modeling of hydrological time series [7], and model forecasting [8, 9]. In this paper, section II presents error source and mathematical model. In section III, we apply ANFIS (adaptive neuro-fuzzy inference system) to model and forecast the compensation error from an unformulated cluster of data. Finally, conclusion and further work are in section IV.

II. ERROR SOURCE AND MODEL ANALYSIS

In each capsule, a compact size encoder is fixed on the bearing housing with a magnet attached on the shaft, which should be positioned centrally and aligned directly over the axis. However, the gap between the inner ring and outer ring introduces some discrepancy in the assembly and results in axis alignment error. In addition, the sensor signal can be affected by EMC (electromagnetic compatibility) disturbance, which can cause missing or extra counts in the signal. Mechanical factors causing erroneous signals include:

- Coupling is not tight and slipping.
- Slippage and correct tension when no belt is used.
- Incorrect wheel for the application or working incorrectly.

- Bad bearings causing roughness or side movement when turning the encoder shaft and thus erratic readings.

The pitch joint angle error of segment 4 is shown in Figure 2. It runs as a retrieve turn from 0° to $+45^\circ$ and reverses to -45° then forward to 0° . The sample period is united time; the rotation speed is set as $1^\circ/s$. It is clear that the forward and retrieve movements have very different result. The data takes on a disclosed hysteresis loop form aligned to a certain amplitude region. When the joint rotates in different direction the curve goes to a multi-trail, i.e. in positive area the forward and backward curve have similar shape, but in negative area the forward and backward curve are widely divergent. Especially on the edge around angular -45° , there is a gap about 0.2° , which indicates unregulated nonlinear components with significant discontinuities.

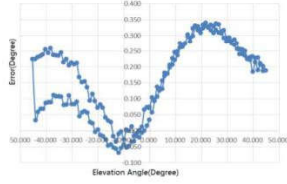


Fig. 2. Pitch Joint Angle Error.

III. PITCH JOINT ERROR ESTIMATOR DESIGN AND TEST

ANFIS differs from normal fuzzy logic systems by the adaptive parameters, i.e., both the premise parameters and the consequent parameters are adjustable. The most noteworthy feature of ANFIS is its hybrid learning algorithm. The adaptation process of the parameters of ANFIS is divided into two steps. In the first step of the consequent parameters training, the Least Mean Squares method (LMS) is used, because the output of ANFIS is a linear combination of the consequent parameters. The second step, the premise parameters. After the consequent parameters have been adjusted, the approximation error is back-propagated BP through every layer to update the premise parameters. This part of the adaptation procedure is based on the gradient descent principle, which is the same as in the training of the Back Propagation (BP) neural network. ANFIS has the rule base: if x is A_i , y is B_j and z is C_k , then $f_{ijk} = \alpha_{ijk}x + \beta_{ijk}y + \theta_{ijk}z + g_{ijk}$. Let the triangular membership functions of fuzzy sets A_i , B_j , C_k $i=1,2, j=1,2,3, k=1,2,3$, has the below form. When the premise parameters are fixed, the overall output is a linear combination of the consequent parameters. In symbols, the output f can be written as which is linear in the consequent parameters $[a \ \beta \ \theta \ g]_{ijk}$ ($i = 1,2, j = 1,2,3, k=1,2,3$). Three input eight rule Sugeno model ANFIS architecture is illustrated in Figure 3.

Layer 1 (2): for each input, the node generates the membership grades of a linguistic label. In (1) $\{a, b, c\}$ is the parameter set. As the values of the parameters change, the shape of the triangular-shaped function varies. Parameters in that layer are called premise parameters. Layer 2 (3): each node calculates the firing strength of each rule using the min or prod operator. In general, any other fuzzy AND operation can be

used. Layer 3 (4): the nodes calculate the ratios of the firing strength of the rule to the sum of the firing strength of all the rules. The result is a normalized firing strength. Layer 4 (5): the nodes compute a parameter function on the layer 3 output. Parameters in this layer are called consequent parameters. Layer 5 (6): a single node aggregates the overall output as the summation of all incoming signals.

$$\text{triangular}(X; a, b, c) = \begin{cases} 0, & X - b \leq X \leq a, \\ \frac{X - a}{b - a}, & a \leq X \leq b, \\ \frac{c - X}{c - b}, & b \leq X \leq c, \\ 0, & c \leq X \end{cases} \quad (1)$$

$$o_i^2 = \mu_{A_i}(x) \times \mu_{B_j}(y) \times \mu_{C_k}(z), i = 1,2, j = 1,2,3, k = 1,2,3 \quad (2)$$

$$\bar{o}_i^2 = w_{i,j,k} \times \mu_{A_i}(x) \times \mu_{B_j}(y) \times \mu_{C_k}(z), i = 1,2, j = 1,2,3, k = 1,2,3 \quad (3)$$

$$o_i^3 = \bar{w}_{i,j,k} = \frac{w_{i,j,k}}{\sum_{i,j,k=1}^8 w_{i,j,k}}, i = 1,2, j = 1,2,3, k = 1,2,3 \quad (4)$$

$$o_i^4 = \bar{w}_{i,j,k} f_{i,j,k} = \bar{w}_{i,j,k} (\alpha_{ijk}x + \beta_{ijk}y + \theta_{ijk}z + g_{ijk}), i = 1,2, j = 1,2,3, k = 1,2,3 \quad (5)$$

$$o_i^5 = \frac{\sum_{i,j,k=1}^8 \bar{w}_{i,j,k} f_{i,j,k}}{\sum_{i,j,k=1}^8 \bar{w}_{i,j,k}}, i = 1,2, j = 1,2,3, k = 1,2,3 \quad (6)$$

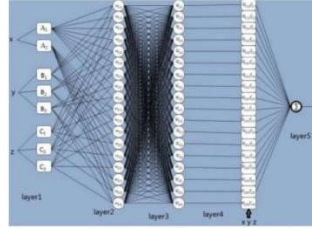


Fig. 3. Three input eight rules Sugeno model ANFIS architecture.

Hybrid algorithm adjusts the consequent parameters in a forward pass and the premise parameters in a backward pass. Because the update rules for the premise and consequent parameters are decoupled in the hybrid learning rule, a computational speedup may be possible by using variants of the gradient method or other optimization techniques on the premise parameters. In the forward pass, the algorithm uses the least squares method to identify the consequent parameters on the layer 4. In the backward pass, the errors are propagated backward and the premise parameters are updated by gradient descent. It is a very powerful approach including the following steps:

- Selection of the fuzzy model type.
- Selection of the Model input and output variables.

- Identification of the fuzzy model structure. This includes determination of the number and types of membership functions for the input and output variables and the number of fuzzy rules.
- Identification of the antecedent and consequent membership function parameters.
- Identification of the consequent parameters of the fuzzy rule base.

In Figure 4(a), stars and circles refer to the training and checking data respectively. Training data model is from about 100 groups of measurement clusters. The checking data we show is under extreme circumstances, which has a heavy distribution. Since the hybrid method is computationally efficient, ANFIS can usually generate satisfactory results after only several epochs of training. After the second application of the least square model, the best performance RMSE error 0.0982 is achieved. In Figure 4(b), the plot shows the checking data as dots and the training data is given as stars. ANFIS chooses the model parameters associated with the minimum checking error. The testing data have an average test error of 0.019696 after 40 epochs, the checking error decreases up to a certain point in the training and then it increases, which represents the point of model overfitting. ANFIS training completed at epoch 2, with minimum checking error 0.100052, which appears in the third epochs. Figure 4(c) displays the desired curve and prediction with the minimal average checking error, which reached 0.017486; the performance for time index from 0 to 177 is better since this is the domain from which the training data was extracted. When some point is missing, or heavily corrupted by noise, the prediction stability can still be hold well. As in Figure 5, laboratory test bench for ANFIS estimator and solution performance of hundreds test are demonstrated.

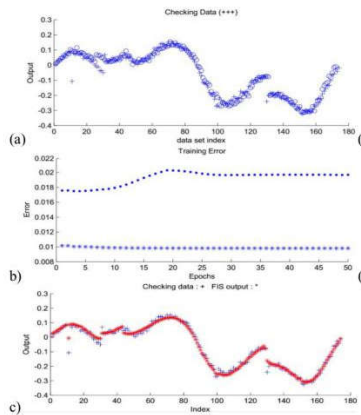
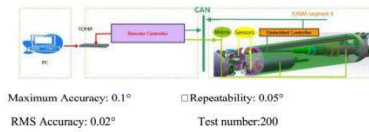


Fig. 4. (a) Training data and checking data distribution. (b) Training (star) and checking (dot) Error curve for 40 epochs. (c) Test data prediction result compare to training data.

IV. CONCLUSION

Compared to yaw joint angle measurement [10], pitch joint shows less regularity and more uncertainty. Software sensor calibration is an attractive solution in our case, where there is little tolerance as regards cost and reliability. This work developed a ANFIS estimator, and applied this algorithm to yaw joint calibration for tracking of errors and implementation of compensation actions. This algorithm is also available in hardware application for a cheaper or less power consumption target. The further work will focus on motion control and vibration damping based on the current result to improve the control performance of EAMA robot.

Fig. 5. Laboratory test bench for ANFIS estimator and test result.



ACKNOWLEDGMENT

The authors would like to express their deepest gratitude to all, whose kindness and advice have made this work possible. We deeply thank colleagues at Institute of Plasma Physics for their hard work and beneficial discussions.

REFERENCES

- [1] E. Dorveaux, D. Vissière, "Iterative calibration method for inertial and magnetic sensors", 48th IEEE Conference on Decision and Control.
- [2] G. Cooper, I. Sheret, "Inertial sensor-based knee flexion/extension angle estimation", *J. Biomechanics*, vol. 42(16), pp.2678–2685, 2009.
- [3] J. Hol, "Sensor Fusion and Calibration of Inertial Sensors, Vision, Ultra-Wideband and GPS", Department of Electrical Engineering, Linköping University, Sweden, 2011.
- [4] P. Eberhard, Q. Tang, "Sensor Data Fusion for the Localization and Position Control of One Kind of Omnidirectional Mobile Robots", *Multibody System Dynamics, Robotics and Control*, pp. 45-73.
- [5] E. Hristoforou, H. Chiria, "On the calibration of position sensors based on magnetic delay lines", 1st European magnetic sensors and actuators conference, *Sensors and Actuators A: Physical*, Vol. 59, pp.89-93, 1997.
- [6] N. Kovac, S. Bauk, "The Anfis based route preference estimation in sea navigation", *Journal of Maritime Research*, vol. 3, pp.69-86, 2006.
- [7] M. Banut, R. Demir, E. Zerdali, "Real-Time Implementation of Bi Input-Extended Kalman Filter-Based Estimator for Speed-Sensorless Control of Induction Motors", *IEEE Transactions on Industrial Electronics*, vol. 59, pp. 4197 - 4206, November 2012.
- [8] A. Akrad, M. Hilairet, D. Diallo, "A sensorless PMSM drive with a two stage extended Kalman estimator", 34th Annual Conference of IEEE Industrial Electronics, pp. 10-13, November, 2008.
- [9] A. Jiménez, B. M. Al-Hadithi, F. Matia, "Extended Kalman Filter for the Estimation and Optimal Control of Takagi-Sugeno Fuzzy Model, In: *Fuzzy Control. Theory*, pp.91-110, 2011.
- [10] J. Wu, Y. Song, "Extended Kalman Filter Estimator with Curve Fitting Calibration of EAST Articulated Maintenance Arm Position Disturbance Compensation", 2016 IEEE International Conference on Electronic Information and Communication Technology.

Publication IV

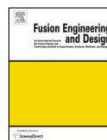
Jing, W., Huapeng, W., and Yuntao, S.
Open software architecture for east articulated maintenance arm

Reprinted with permission from
Fusion Engineering and Design
Vol. 109-111, pp. 474-479, 2016
© 2016, Elsevier



Contents lists available at ScienceDirect

Fusion Engineering and Design

journal homepage: www.elsevier.com/locate/fusengdes

Open software architecture for east articulated maintenance arm

Jing Wu^{a,b,*}, Huapeng Wu^b, Yuntao Song^a, Ming Li^b, Yang Yang^a, Daniel A.M. Alcina^b^a Institute of Plasma Physics Chinese Academy of Sciences, 350 Shushanhu Rd Hefei Anhui, China^b Lappeenranta University of Technology, Skinnarilankatu 34 Lappeenranta, Finland

HIGHLIGHTS

- A software requirement of serial-articulated robot for EAST assembly and maintains is presented.
- A open software architecture of the robot is developed.
- A component-based model distribution system with real-time communication of the robot is constructed.

ARTICLE INFO

Article history:

Received 31 August 2015

Received in revised form 13 February 2016

Accepted 22 February 2016

Available online 28 February 2016

Keywords:

EAST

EAMA

Maintenance

Software architecture

Real-time control

OROCOS

ABSTRACT

For the inside inspection and the maintenance of vacuum vessel in the EAST, an articulated maintenance arm is developed. In this article, an open software architecture developed for the EAST articulated maintenance arm (EAMA) is described, which offers a robust and proper performance and easy-going experience based on standard open robotic platform OROCOS. The paper presents a component-based model software architecture using multi-layer structure: end layer, up layer, middle, and down layer. In the end layer the components are defined off-line in the task planner manner. The components in up layer complete the function of trajectory plan. The CORBA, as a communication framework, is adopted to exchange the data between the distributed components. The contributors use Real-Time Workshop from the MATLAB/Simulink to generate the components in the middle layer. Real-time Toolkit guarantees control applications running in the hard real-time mode. Ethernets and the CAN bus are used for data transfer in the down layer, where the components implement the hardware functions. The distributed architecture of control system associates each processing node with each joint, which is mapped to a component with all functioning features of the framework.

© 2016 Elsevier B.V. All rights reserved.

1. Introduction

The Institute of Plasma Physics Chinese Academy of Sciences has been running the EAST (Experimental Advanced Superconducting Tokamak) project since 2000, which targets on the development of a small non-circular cross-section superconductor tokamak and its subsystems. The EAST articulated maintenance arm (EAMA) subsystem project began from 2013, which is aimed to implement the remote handling operations in the EAST for the routine inspection and maintenance. To date, some sorts of teleoperation manipulator applications, for example the ITER Articulated Inspection Arm (AIA) [1], the Planar Articulated Arm (PAA), the ITER Mobile Parallel Robot [2] and the Articulated Teleoperated Manipulator (ATM) [3], had been developed. Many of them run on the commercial soft-

ware platforms or the research software prototypes [4], and various applications have been derived from the development, in course of these applications [5], covered the topics of reliable real time control system design, graphical supervisor, and robot localization realistic etc.

The physical EAMA system is shown in Fig. 1, it mainly consists of 3 parts: cask, shuttle, and manipulator, and for each part there are several peripherals. Fig. 2 shows the structure of the EAMA, each subsystem elementary technologies are composited individually and integrated into EAMA system model, which makes compatibility and portability the major concerns in software design. The EAMA software is designed based on an open source architecture that favors the capacity and portability demands, and it also offers massive models and algorithms especially pertaining to the long dimension, joint-reductant, structure-flexible manipulator for the purpose of easy approach and long term research.

This paper is focused on software design for the robot represented by the hexagon in Fig. 2 and the paper is structured as

* Corresponding author.

E-mail addresses: wujing@ipp.ac.cn, mirror3@hotmail.com (J. Wu).

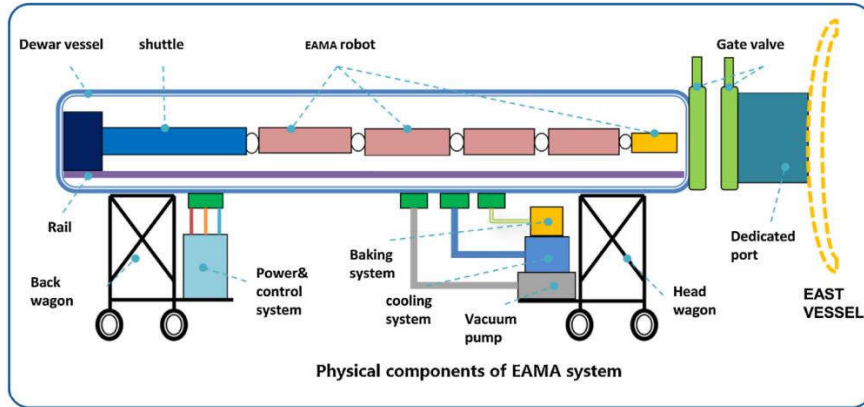


Fig. 1. Physical component of EAMA system.

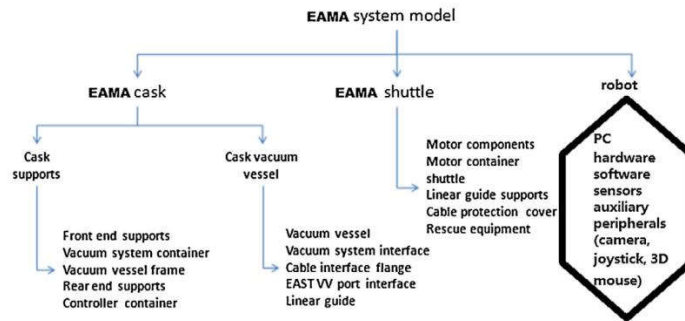


Fig. 2. EAMA system prototype development structure.

follows: Section 2 presents the related work of the robot software, control system prototype of other tokamak system and the objectives of current software solutions; Section 3 gives the overview of software attributes, software distribution system, software configuration, supervisor, visualization, layers, components distributions, communication, scheduling, hardware abstraction and low-level control. In the last section the conclusion and further work are discussed.

2. Related work

2.1. ITER robotics

The ITER Articulated Inspection Arm (AIA) robot is developed by the Institute for Magnetic Fusion Research (IRFM) [6], the CEA licensed Energid's Actin software to be the AIA robot supervision, which works in collaboration with AREVA and OPEN CASCADE, by a turnkey application layer for intuitively controlling the robot and preventing collisions dynamically. In Shanghai Jiao Tong University, the State Key Laboratory of Mechanical System and Vibration and the Research Institute of Robotics presented a remote handling robot (RHR) system that consist of three parts: an omnidirectional transfer vehicle (OTV), a Planar Articulated Arm (PAA), and an

Articulated Teleoperated Manipulator (ATM) [3]. It is simulated by MATLAB and robot technology middleware (RTM) for a remote operation.

2.2. EAST FIVIR

As shown in Fig. 3, a flexible in-vessel inspection robot (FIVIR) is the outcome of a joint project between the Institute of Plasma Physics in Chinese Academy of Sciences (ASIPP) and the Shanghai Jiao Tong University (SJTU), which is used for carrying servicing facilities in EAST. A multi-body system model of the end-effector is created using ADAMS analysis [7].

2.3. Design objectives

The functions of software architecture of EAMA cover the aspects of task management, communication coordination, movement achievement, etc. The software should achieve the multiple objectivities in the development course, which includes the schedulability, the stability, the portability and the compatibility, elaborated in details as follows:

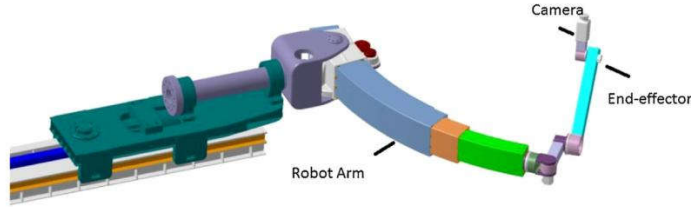


Fig. 3. Flexible in-vessel inspection robot.

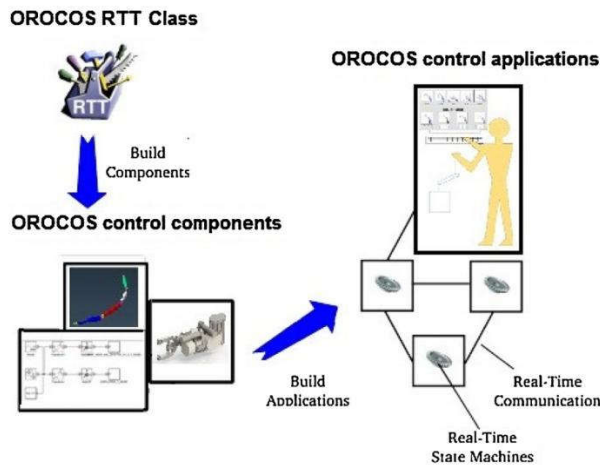


Fig. 4. OROCOS distributed software develops work flow.

Table 1
Demand of software features.

Project application	User experience
Third-party expendable	Haptic device
Easy to migrate to other environments	3D mouse
Available library and standard support	3D Visualization
Fast develop period	Graphical interface
Easy to master code programming	Emergence button
Low budget software prototype	

- **Schedulability:** the tasks in the software can be scheduled in a deterministic way, and for the motion control of EAMA, the real-time schedule ability should be provided.
- **Stability/Robustness:** the software can tolerate the failures in the individual tasks, and it is critical to the robot in the hostile environment.
- **Compatibility** allows the components of the software been developed in different software environment, such as in different languages. The components can be reused by one the other.
- **Portability** enables the software been deployed in different hardware environment. It also friendly allows the alien hardware to join seamlessly.

Beside the above demands, there are other functions required in the project application, and user interfaces related to fusion engineering application are listed in Table 1.

The Open Robot Control Software (OROCOS) is adapted to meet the requirements above. The open software architecture could reduce application budget and testing time, shorten the development period and realize the portability. The OROCOS Real Time Toolkit (RTT) middleware provides utilities to communicate or execute of the components in real-time and guarantee the schedulability, which does not easily crash a process. By using scripting language, it is easy to operate by no experienced programmers. Plenty libraries and standards offer variable control models and peripheral, which have access to GUI, visualization, control devices and plug-ins.

3. Overview of software architecture

The EAMA software is mainly taking care of supervision, visualization, low-level/close-loop control, peripheral device integration, and sensory information streaming, etc.

3.1. Configuration of EAMA software

The concept of component-based software design emphasizes on the construction of system using amount of software model classes [8], as shown in Fig. 4. Considering maximizing the efficiency of the entire application, different components should be able to exchange data and run in different applications. Each composition in the distributed environment shares the data and the

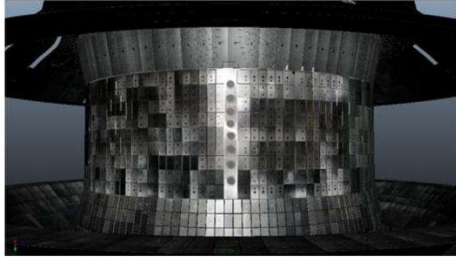


Fig. 5. EAST VV reconstruction scenes.

resources; each component contains many models such as algorithm model, simulation model, estimator model, library model etc. [9]. These open source software packages are integrated with massive operating system and internet communicates through an open standard Common Object Request Broker Architecture (CORBA).

3.2. Supervisor and visualization

The supervisor part of the software of the EAMA contains multiple models for different functions, such as collision avoidance trajectory planning, deformation compensation due to gravity, positioning error compensation, dynamic model simulation and control. The compensation algorithm is employed to compensate the deflection by the effect of gravity and positioning errors, and the algorithm combines the flexible dynamic model in the feedback control during the practical operating process. The trajectory planning takes into account of collision prevention in real-time to achieve the collision free operation. The EAST Vacuum Vessel 3D reconstruction scenes and the EAMA 3D Gazebo simulations are shown in Fig. 5. Fig. 8 shows certain view of the EAMA movement. The component-based distributed software is implementing on the OROCOS platform by using a high level object-oriented language (C++) and a script language Lua integrated in the OROCOS RTT frame-work.

3.3. Layers and components distributions

In the distributed architecture different types of components are distributed and categorized by the concept of abstract layers based on the component's individual functionality, as shown in Fig. 6.

- In the end layer, task planner components are defined off-line in the task planner application, which receives the tasks from user or control device.
- In the up layer, execution components implement the functions of trajectory plan, positioning error compensation computation, dynamic model computation, and control integration, which are computation-exhausting.
- In the middle layer, the control component and the sensor fusion component are generated using the Real-Time Workshop in MATLAB/Simulink, which are running in the hard real-time scheduling.
- In the down layer, the joint control components and sensor components, which are deployed in the embedded system, deal with hardware physical connection to actuators.

3.4. Communication and scheduling

The OROCOS applications have a typical layout of components, as shown in Figs. 7 and 8. The OROCOS adopts the standards

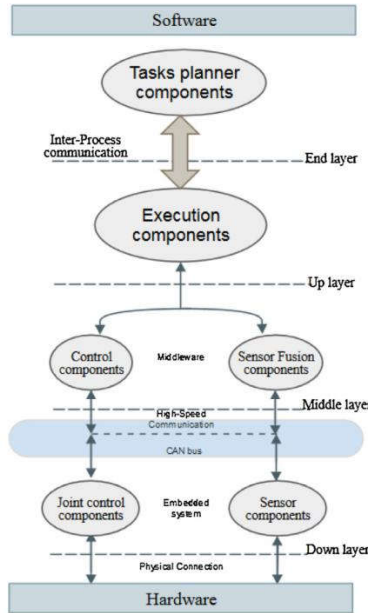


Fig. 6. Components distribution in layers.

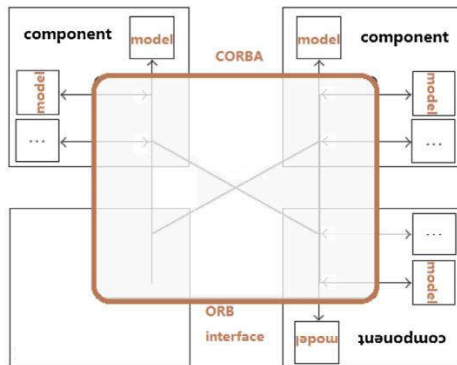


Fig. 7. Communication and scheduling in component models.

and technologies from the CORBA—a communication framework providing maintained bindings, which routes the communication inside a process with the efficiency and real-time performance. Flow ports are taking care of sending the messages resulted from the sensor readings or computation results between the components.

The RTT is a middleware between components and operating system and primitives for task communication. It contains applications for control in hard real-time, and the components generated in MATLAB/Simulink Real Time Workshop. The OROCOS provides real-time state machine for the application supervision

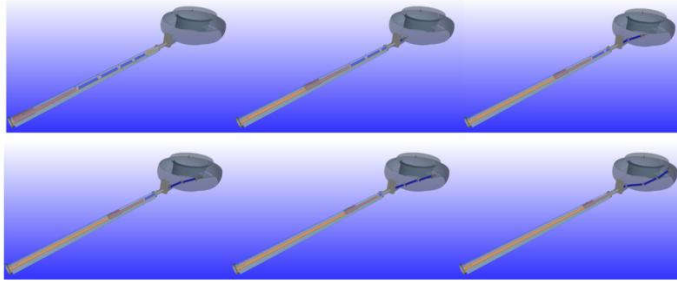


Fig. 8. EAMA 3D Gazebo simulations showing the movement of the maintenance arm into the vacuum vessel, seen from the outside.

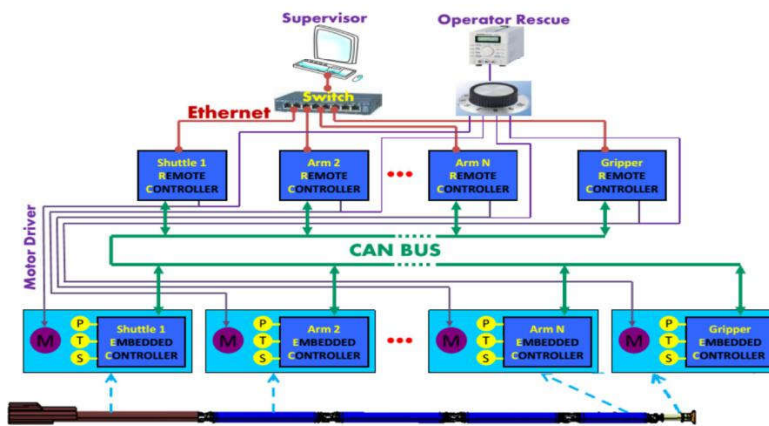


Fig. 9. Hardware configuration of EAMA.

in running time, as well as the life-cycle component, which allows coordinated switch of applications, in emergency or security operation condition.

3.5. Hardware abstraction and low-level control

In Fig. 9, hardware structure from up to down is illustrated, there are two groups of hardware components of the EAMA in charge of the low level control of the manipulator after supervisor sends the control message to the switch. The sensor components are in the form of embedded boards that are integrated in each of the segments of the manipulator and connected in a CAN bus network. The remote controllers connect to the sensor components through the CAN bus and communicate with supervisor through the Ethernet. This hardware layout significantly reduces the wiring required to power and to exchange the data between embedded boards, remote controllers, and supervisor. The remote controllers that are out of the cask and located in a control unit, which contains an emergency system as the backup in case of component damage. It also provides the opportunity to drive the robot into its home position and keep the vacuum vessel free of obstructions.

The close-loop control is implemented by adopting three cascade loops of PID control, e.g., current feedback loop, speed feedback loop, and final position feedback loop. In resume, the high

level control commands are sent to the remote controllers to drive the DC-motors and the feedback signs are obtained via embedded board. The optimized distributed software with high flexibility is easily adapted to the low level hardware, which results in getting smaller, faster, cheaper control board and monitor peripheral. In emergency case, rescue operator would directly connect to the remote controllers that send the brake signal to motor driver, then power off the motor.

5. Discussion, conclusion and future work

The paper presents the open software architecture for EAMA. The conclusions can be summarized as follows:

- First, this new open software architecture allows EAMA to easily incorporate the new sensors and advance control algorithms using a component-based software methodology.
- The connection between the simulator and EAMA is enhanced by employing the real-time communication through open standard CORBA and RTAI with OROCOS RTT and Real-Time Workshop from MATLAB/Simulink.
- Together with the component-based model and distribution environment, a layered software structure has been proposed to embody the design; this structure brings the systems of com-

ponents a standardized interface that connects the components while help the developer be away from the implementation of component details. This feature can make the development of the controllers more efficient and the developed controllers more reliable.

Since the foundation of EAMA software is constructed, the further work focus on general artificial intelligent model design and increasing the third-party library or plug-in numbers to achieve more complex tasks, which could enhance the EAMA agile ability for an entire automation demand in future.

Acknowledgments

This project is supported by Chinese ITER Special Support Project, No. 2014GB101000. We deeply thank to colleagues of Lappeenranta University of Technology for their hard work and beneficial discussions.

References

- [1] Laurent Gargiulo, Pascal Bayetti, Vincent Bruno operation of an ITER relevant inspection robot on tore supra tokamak, *Fusion Eng. Des.* 84 (2009) 220–223.
- [2] Yongbo Wang, Pekka Pessi, Huapeng Wu, Heikki Handroos, Accuracy analysis of hybrid parallel robot for the assembling of ITER, *Fusion Eng. Des.* 84 (2009) 1964–1968.
- [3] Peihua Chen, Qixin Cao, Development of a remote handling robot for the maintenance of an ITER-like D-shaped vessel, *Sci. Technol. Nucl. Install.* (2014) 1–9.
- [4] Yann Perrot, Laurent Gargiulo, Michael Houry, Long-reach articulated robots for inspection and mini-invasive interventions in hazardous environments: recent robotics research, qualification testing, and tool developments, *J. Field Robot.* 29 (1) (2012) 175–185.
- [5] Delphine Keller, P. Bayetti, J. Bonnemason, V. Bruno, Real time command control architecture for an ITER relevant inspection robot in operation on Tore Supra, *Fusion Eng. Des.* 84 (2009) 1015–1019.
- [6] <http://www.prnewswire.com/news-releases/energids-actin-control-software-enables-nuclear-inspection-robot-in-china-300120102.html>.
- [7] Xuebing Peng, Jianjun Yuan, Weijun Zhang, Yang Yang, Yuntao Song, Kinematic and dynamic analysis of a seriallink robot for inspection process in EAST vacuum vessel, *Fusion Eng. Des.* 87 (5–6) (2012) 905–909.
- [8] Lin Zhang, Peter Sjaets, Herman Bruyninckx, An open embedded industrial robot hardware and software architecture applied to position control and visual servoing application, *Int. J. Mechatron. Autom.* 4 (2014) 63–72, No.1.
- [9] H. Bruyninckx, Open robot control software: the orocos project IEEE international conference on robotics and automation, *Proceedings 2001 ICRA 3* (2001) 2523–2528.

Publication V

Jing, W., Huapeng, W., and Yuntao, S.

Adaptive Neuro-fuzzy inference system based estimation of EAMA elevation joint error compensation

Reprinted with permission from
Fusion Engineering and Design
Vol. 126, pp. 170-173, 2018
© 2018, Elsevier



Contents lists available at ScienceDirect

Fusion Engineering and Design

journal homepage: www.elsevier.com/locate/fusengdes

Adaptive Neuro-fuzzy inference system based estimation of EAMA elevation joint error compensation

Jing Wu^{a,b,*}, Huapeng Wu^b, Yuntao Song^a, Tao Zhang^a, Jun Zhang^a, Yong Cheng^a^a Institute of Plasma Physics Chinese Academy of Sciences, 350 Shushanhu Rd, Hefei Anhui, China^b Lappeenranta University of Technology, Skinnarilankatu 34 Lappeenranta, Finland

ARTICLE INFO

Keywords:
EAST
EAMA
Neuro-fuzzy
Estimator
Incremental encoder
Calibration

ABSTRACT

EAMA (EAST Articulated Maintenance Arm) is an articulated serial robot arm working in experimental advanced superconductor tokamak for the inspection and maintenance. This paper implements algorithms to calibrate the synchronize deflection and estimate its signal for the robot control. The retrieval has two distinct tasks, a shaft rotation direction signal processing and a discrete data classification, meanwhile neuro network and expert system are applied for completing these separate tasks respectively. In this paper the use of Adaptive Neuro-fuzzy Inference System for estimating the compensation error from an unformulated cluster of data that has unneglectable nonlinearity is presented. The simulation result shows that the root mean squared error is significant improved, the final results satisfy the accuracy.

1. Introduction

EAMA (EAST Articulated Maintenance Arm) is a long articulated flexible robot for the experimental advanced superconductor tokamak vacuum vessel (VV) [1]. Its maintenance services include geometrically enclosed space inspection and graphite tile friction cleaning for the Plasma Facing Components (PFCs) of the EAST vessel [2]. As shown in Fig. 1, this segment composites with a rotation and elevation joints, for such complex mechanisms the accurate and reliable operations in work space are required [3]. It is not always easy to acquire the exact model from the sensed results to manage the remotely control by using error compensation. The use of intelligent hybrid system is growing rapidly with successful applications in process control, especially for model-less application. In most case, the Adaptive Neuro-fuzzy Inference System (ANFIS) architecture is employed to model nonlinear functions, estimate nonlinear components in on-line control system, and forecast a chaotic time series, which produce significant improvement in the results [4]. Many researches have been applied on ANFIS senseless estimation [5], modeling hydrological time series [6], model forecasting [7,8]. For rotation, Extended Kalman Filter has been adopted to estimate the compensation error in the curve fitted idealized model of the difference between reference data and experiment measurement [9]. However for elevation, it is more suitable to use Adaptive Neuro-fuzzy Inference System modeling and forecasting the error in EAMA joints.

This paper presents the use of Adaptive Neuro-fuzzy Inference System to estimate the compensation error from an unformulated

cluster of data. First, two distinct sub-tasks, shaft rotation direction signal processing and serial data modeling are presented then neuro network and expert system are investigated to solve these separate tasks respectively. After this introduction, the rest of the paper is organized as follows: Section 2 formulates the target model analysis, error sources. Section 3, 4 present Adaptive Neuro-fuzzy Inference System algorithm strategy, objectives and test results. Finally, the last section outlines the main conclusions.

2. Error source and model analysis

In the segment 4 of the manipulator there are two AS5047D incremental sensors, which are illustrated in Fig. 2(a) [10]. The microchip is fixed on the bear housing and the magnet is attached to the shaft, which axis of the magnet must be aligned on the center of the package as shown in Fig. 2(b). As the assembly error in the gap between the inner ring and outer ring, it results a difficulty of axis aligning when rotor is running. When the Anti-rotational mounting of the encoder is not proper, the missing or extra counts could be caused by the mechanical factor listed below [11].

- Coupling is not tight and slipping.
- Slippage and incorrect tension could happen, when belt is used.
- Incorrect wheel for the application or working incorrectly.
- Roughness or side movement turning encoder shaft can mean a bad bearings, which can cause erratic readings.

* Corresponding author at: Institute of Plasma Physics Chinese Academy of Sciences, 350 Shushanhu Rd, Hefei Anhui, China.
E-mail addresses: WuJing@ipp.ac.cn, mirror_a3@hotmail.com, songyt@ipp.ac.cn (J. Wu).

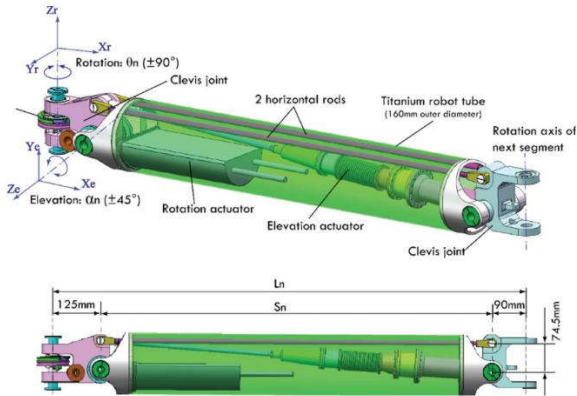


Fig. 1. EAMA segment prototype mechanism structure.

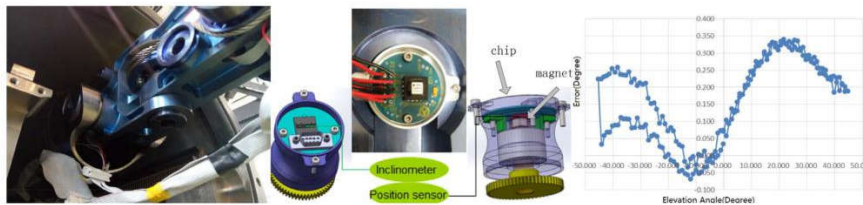


Fig. 2. (a) Joint structure, (b) Mechanical installation of ASS047D, (c) Elevation Angle Error.

We measured a retrieve turn from 0° to +45° and travel inverse to -45° then back to 0°. The sample period is united from reference encoder and demo board. The rotation speed is settled to 1° per second. The results of segment 4 drawn in Fig. 2(c) are aligned to a certain amplitude region, which adhere to unregulated non-linearity with a significant discontinuous. This data model is hard to be curve fitted or data driven. The intelligent artificial algorithm is always an available option to solve this problem.

3. Adaptive Neuro-fuzzy inference system

3.1. Neuro network and fuzzy system

Fuzzy logic provides a mathematical ability to capture the sort of uncertainties associated with cognitive processes, which is difficult to acquire from increment measurement. Artificial neuro systems can be understood as simplified mathematical model of learning systems and they work as parallel distributed computing networks (Table 1).

3.2. Adaptive Neuro-fuzzy inference system

The ANFIS is a class of adaptive network [12], which is functionally

Table 1 Comparison of neuro network and fuzzy system.

Neuro Networks	Fuzzy Systems
no mathematical model necessary	no mathematical model necessary
learning from scratch	priori knowledge essential
several learning algorithms	not capable to learn
black-box behavior	simple interpretation and implementation

Table 2 ANFIS Pseudo-Code.

Pseudo-code of ANFIS
Set (Number Of Inputs, 3);
Set (Number Of Outputs,1);
Set (Number Of MF,2, 3, 3);
Set (Type of MF, trimf)
For input: = 1 to Number Of Inputs do
Begin
Read (TrainingData);
Determine (TrainingDataNumber);
Calculate (NumberOfRules);
Identifying (antecedent, consequent);
Identifying (consequent parameters);
CreateRules;
Set (EpochNumber,40);
Learning;
Testing;
End

equivalent to FISs. The basics of ANFIS are introduced in detail in many mathematical related research [13–15]. As the pseudo code shown in Table 2, it is a very powerful approach for building complex and non-linear relationship between a set of input and output data sets, which includes the follow issues[16].

- Fuzzy model type selection.
- Model input and output variables selection.
- Fuzzy model structure identification, which includes determination of the number and types of membership functions for the input and output variables and the number of fuzzy rules.
- Antecedent and consequent membership functions parameters identification.

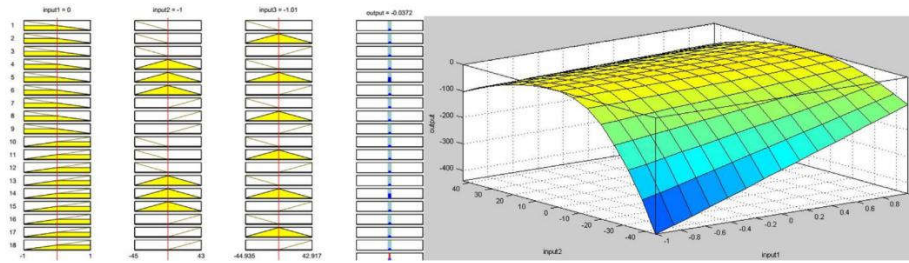


Fig. 3. (a) Triangular-shaped membership function. (b) ANFIS surface for error prediction.

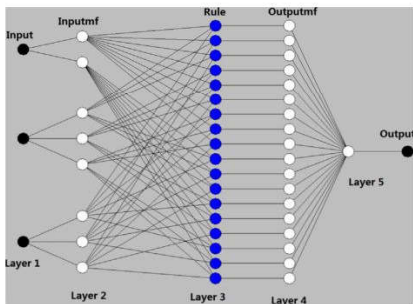


Fig. 4. Architecture of the ANFIS models.

- Identifying the consequent parameters of the fuzzy rule base.

ANFIS applies the Sugeno fuzzy model, due to its high interpretability and computational efficiency. It starts with initialize the input, output, member function, member function type, then begins to provide initial conditions for posterior ANFIS training.

It was assumed that the EAMA sensor calibration under consideration has three inputs: rotation direction, commend reference, and sensed data; and one output, which needs error compensation. The numbers of membership functions (MFs) for the inputs are [2, 3, 3]. The fuzzy theory with respect to the traditional logic theory, which an element can belong or not to a particular set, allows the partial membership of an element to a set. For input 1, it has only two value clockwise or counter clockwise as [-1, 1]. Input 2 refers from 0° to 43°, retrieve to -45°, and then travel back to 0°. As shown in Fig. 3(a), each value of the variables is characterized by a triangular-shaped membership, which changes with continuity from zero to one. The

membership function for each variable establishes the rate at a certain set. Fig. 3(b) cut off at the maximum and minimum of the desired output.

The architecture of the ANFIS model is shown in Fig. 4, in which a colored circle indicates a fixed node, where the white circle indicates an adaptive node. For a first-order Sugeno fuzzy model, a common rule set with eighteen (2*3*3) fuzzy, which has listed below.

- Number of nodes: 58
- Number of linear parameters: 72
- Number of nonlinear parameters: 24
- Total number of parameters: 96
- Number of training data pairs: 172
- Number of checking data pairs: 174
- Number of fuzzy rules: 18

3.3. EAMA evolution joint calibration algorithm test

In Fig. 5, two groups of data have been illustrated as star and circular, which refers to the training and testing data. Training data model is from about 50 groups of measurement cluster. In the distribution most of the test data follows the base model, but some data is clearly inaccurate. Compare to rotation angle measurement [9], Revelation joint shows less regularity and more uncertainty, the candidate inputs are divided into three sets due to physical properties. Since the hybrid (mixed least-squares and back propagation) method is computationally efficient, ANFIS can usually generate satisfactory results right after several epochs of training. After the second application of the least square model, we choose one with the best performance RMSE error is 0.0982 and proceed for further training.

In Fig. 6, testing data finally have the average test error 0.019696 after 40 epochs, but the test minimal error appears in the third epochs and also designated epoch number reached, that ANFIS training completed at epoch 2, with training data error 0.100052. Fig. 7 displays the desired curve and ANFIS prediction, with the test minimal error which

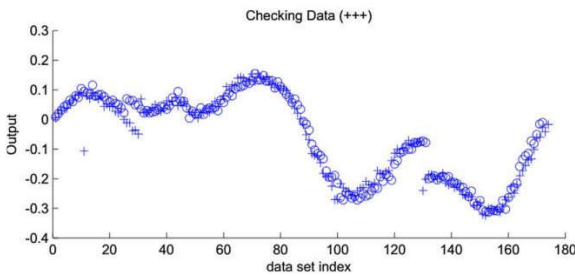


Fig. 5. Training data and Checking data distribution.

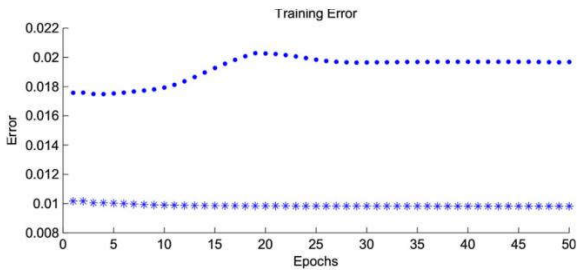


Fig. 6. Training (star) and testing (dot) error curve for 40 epochs.

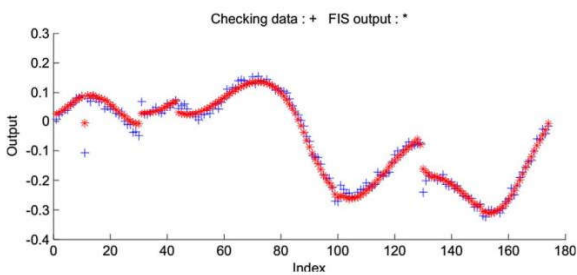


Fig. 7. Test data prediction result compare to training data.

reached 0.017486; the performance for time index from 0 to 177 is better, since this is the domain from, which the training data was extracted. When some point is missing, or over disturbed, the prediction stability can still be hold well.

4. Discussion, conclusion and future work

When we compare to the previous work of EAMA [9], it is clear to have many summaries of advantages in ANFIS for error estimation and sensor calibration, which can be concluded as follows.

- ANSFI architecture allows EAMA to easily incorporate the non-mathematical model sensors calibration and advance control algorithms.
- The training process usually only takes few epochs, which shorten the calculation time and satisfied the accuracy requirement
- ANFIS models for various combinations of inputs, train them with a single application for certain types of problems. Since the candidate inputs are divided into groups by data structure, one or several members of each group can be added in the set of final inputs to the model under consideration. It bring more flexibility to modify the sensor calibration factor, or even combine with other application, which allow us to build less potential EAMA models initially.

Since the requirement of EAMA sensing accuracy is reached, the further work focus on motion control and vibration damping based on current result. Later the research of EAMA force feedback and dynamic feed-forward control system will be carried on.

Acknowledgments

This project is supported by Chinese ITER Special Support Project, No. 2014GB101000. We deeply thank to colleagues of Lappeenranta

University of Technology for their hard work and beneficial discussions

References

- [1] J. Wu, H. Wu, Y. Song, et al., Open software architecture for EAST articulated maintenance arm, Fusion Eng. Des. 109–111 (2016) 474–479.
- [2] J. Wu, H. Wu, Y. Song, et al., Genetic algorithm trajectory plan optimization for EAMA: EAST articulated maintenance arm, Fusion Eng. Des. 109–111 (2016) 700–706.
- [3] L. Lin, Y. Song, Y. Yang, H. Feng, Computer vision system R&D for EAST articulated maintenance arm robot, Fusion Eng. Des. 100 (920–3796) (2015) 254–259.
- [4] J. Jang, ANFIS: adaptive-network-based fuzzy inference systems, IEEE Trans. Syst. Man Cybern. 23 (3) (1993) 665–685.
- [5] F. Lima, W. Kaiser, I.N.D. Silva, Speed Neuro-fuzzy estimator for sensorless indirect flux oriented induction motor drive, Conference of the IEEE Industrial Electronics Society (2010) 2926–2931.
- [6] P.C. Nayak, K.P. Sudheer, D.M. Rangan, et al., A Neuro-fuzzy computing technique for modeling hydrological time series, J. Hydrol. 291 (1–2) (2004) 52–66.
- [7] Z. He, X. Wen, H. Liu, et al., A comparative study of artificial neural network, adaptive neuro fuzzy inference system and support vector machine for forecasting river flow in the semiarid mountain region, J. Hydrol. 509 (529) (2014) 379–386.
- [8] N. Kovac, S. Bauk, The anfis based route preference estimation in sea navigation, J. Maritime Res. 3 (2006) 69–86.
- [9] J. Wu, Y. Song, Y. Jian, Extended Kalman filter estimator with curve fitting calibration of EAST articulated maintenance arm position disturbance compensation, 2016 IEEE International Conference on Electronic Information and Communication Technology, August 20–22 (2016).
- [10] <http://ams.com/eng/Products/Magnetic-Position-sensors/Angle-PositionOn-Axis/AS5047D>.
- [11] <http://encoder.com/literature/troubleshooting-guide.pdf>.
- [12] https://en.wikipedia.org/wiki/Adaptive_neuro_fuzzy_inference_system.
- [13] J. Moon, J. Chang, S. Kim, Determining adaptability performance of artificial neuro network-based thermal control logics for envelope conditions in residential buildings, Energies 6 (7) (2013) 3548–3570.
- [14] J. Jang, Input selection for ANFIS learning, IEEE Int. Conf. Fuzzy Syst. 2 (1996) 1493–1499.
- [15] A. Depari, A. Flammini, D. Marioli, A. Taroni, Application of an ANFIS algorithm to sensor data processing, IEEE Instrum. Meas. Technol. Conf. 56 (1) (2007) 75–79.
- [16] A. Abraham, Y. Jarraya, S. Bouaziz, Fuzzy modeling system based on hybrid evolutionary approach, International Conference on Hybrid Intelligent Systems 2013 (2013) December.

ACTA UNIVERSITATIS LAPPEENRANTAENSIS

752. SHI, SHANSHUANG. Development of the EAST articulated maintenance arm and an algorithm study of deflection prediction and error compensation. 2017. Diss.
753. CHEN, JIE. Institutions, social entrepreneurship, and internationalization. 2017. Diss.
754. HUOTARI, PONTUS. Strategic interaction in platform-based markets: An agent-based simulation approach. 2017. Diss.
755. QU, BIN. Water chemistry and greenhouse gases emissions in the rivers of the "Third Pole" / Water Tower of Asia". 2017. Diss.
756. KARHU, PÄIVI. Cognitive ambidexterity: Examination of the cognitive dimension in decision-making dualities. 2017. Diss.
757. AGAFONOVA, OXANA. A numerical study of forest influences on the atmospheric boundary layer and wind turbines. 2017. Diss.
758. AZAM, RAHAMATHUNNISA MUHAMMAD. The study of chromium nitride coating by asymmetric bipolar pulsed DC reactive magnetron sputtering. 2017. Diss.
759. AHI, MOHAMADALI. Foreign market entry mode decision-making: Insights from real options reasoning. 2017. Diss.
760. AL HAMDY, ABDULLAH. Synthesis and comparison of the photocatalytic activities of antimony, iodide and rare earth metals on SnO₂ for the photodegradation of phenol and its intermediates under UV, solar and visible light irradiations. 2017. Diss.
761. KAUTTO, JESSE. Evaluation of two pulping-based biorefinery concepts. 2017. Diss.
762. AFZALIFAR, ALI. Modelling nucleating flows of steam. 2017. Diss.
763. VANNINEN, HEINI. Micromultinationals - antecedents, processes and outcomes of the multinationalization of small- and medium-sized firms. 2017. Diss.
764. DEVIATKIN, IVAN. The role of waste pretreatment on the environmental sustainability of waste management. 2017. Diss.
765. TOGHYANI, AMIR. Effect of temperature on the shaping process of an extruded wood-plastic composite (WPC) profile in a novel post-production process. 2017. Diss.
766. LAAKKONEN, JUSSI. An approach for distinct information privacy risk assessment. 2017. Diss.
767. KASURINEN, HELI. Identifying the opportunities to develop holistically sustainable bioenergy business. 2017. Diss.
768. KESKISAARI, ANNA. The impact of recycled raw materials on the properties of wood-plastic composites. 2017. Diss.
769. JUKKA, MINNA. Perceptions of international buyer-supplier relational exchange. 2017. Diss.
770. BAYGILDINA, ELVIRA. Thermal load analysis and monitoring of doubly-fed wind power converters in low wind speed conditions. 2017. Diss.
771. STADE, SAM. Examination of the compaction of ultrafiltration membranes with ultrasonic time-domain reflectometry. 2017. Diss.

772. KOZLOVA, MARIIA. Analyzing the effects of a renewable energy support mechanism on investments under uncertainty: case of Russia. 2017. Diss.
773. KURAMA, ONESFOLE. Similarity based classification methods with different aggregation operators. 2017. Diss.
774. LYYTIKÄINEN, KATJA. Removal of xylan from birch kraft pulps and the effect of its removal on fiber properties, colloidal interactions and retention in papermaking. 2017. Diss.
775. GAFUROV, SALIMZHAN. Theoretical and experimental analysis of dynamic loading of a two-stage aircraft engine fuel pump and methods for its decreasing. 2017. Diss.
776. KULESHOV, DMITRII. Modelling the operation of short-term electricity market in Russia. 2017. Diss.
777. SAARI, JUSSI. Improving the effectiveness and profitability of thermal conversion of biomass. 2017. Diss.
778. ZHAO, FEIPING. Cross-linked chitosan and β -cyclodextrin as functional adsorbents in water treatment. 2017. Diss.
779. KORHONEN, ILKKA. Mobile sensor for measurements inside combustion chamber – preliminary study. 2017. Diss.
780. SIKIÖ, PÄIVI. Dynamical tree models for high Reynolds number turbulence applied in fluid-solid systems of 1D-space and time. 2017. Diss.
781. ROMANENKO, ALEKSEI. Study of inverter-induced bearing damage monitoring in variable-speed-driven motor systems. 2017. Diss.
782. SIPILÄ, JENNI. The many faces of ambivalence in the decision-making process. 2017. Diss.
783. HAN, MEI. Hydrodynamics and mass transfer in airlift bioreactors; experimental and numerical simulation analysis. 2017. Diss.
784. ESCALANTE, JOHN BRUZZO. Dynamic simulation of cross-country skiing. 2017. Diss.
785. NOKKA, JARKKO. Energy efficiency analyses of hybrid non-road mobile machinery by real-time virtual prototyping. 2018. Diss.
786. VUORIO, ANNA. Opportunity-specific entrepreneurial intentions in sustainable entrepreneurship. 2018. Diss.
787. PULKKINEN, AKI. Towards a better understanding of activity and selectivity trends involving K and O adsorption on selected metal surfaces. 2017. Diss.
788. ZHAO, WENLONG. Reliability based research on design, analysis and control of the remote handling maintenance system for fusion reactor. 2018. Diss.
789. IAKOVLEVA, EVGENIA. Novel sorbents from low-cost materials for water treatment. 2018. Diss.
790. KEDZIORA, DAMIAN. Service offshoring industry: systems engineering approach to its transitional challenges. 2018. Diss.

Acta Universitatis
Lappeenrantaensis
791



LUT
Lappeenranta
University of Technology

ISBN 978-952-335-207-0

ISBN 978-952-335-208-7 (PDF)

ISSN-L 1456-4491

ISSN 1456-4491

Lappeenranta 2018
